Published in final edited form as:
J Chem Phys. 2011 August 14; 135(6): 065105. doi:10.1063/1.3608916.

Nucleated polymerization with secondary pathways I. Time evolution of the principal moments

Samuel I. A. Cohen[1], **Michele Vendruscolo**[1], **Mark E. Welland**[2], **Christopher M. Dobson**[1], **Eugene M. Terentjev**[3], and **Tuomas P. J. Knowles**[1]

[1]Department of Chemistry, University of Cambridge, Lensfield Road, Cambridge CB2 1EW, UK

[2]Nanoscience Centre, University of Cambridge, J J Thomson Avenue, Cambridge CB3 0FF, UK

[3]Cavendish Laboratory, University of Cambridge, J J Thomson Avenue, Cambridge CB3 0HE, UK

Abstract

Self-assembly processes resulting in linear structures are often observed in molecular biology, and include the formation of functional filaments such as actin and tubulin, as well as generally dysfunctional ones such as amyloid aggregates. Although the basic kinetic equations describing these phenomena are well-established, it has proved to be challenging, due to their non-linear nature, to derive solutions to these equations except for special cases. The availability of general analytical solutions provides a route for determining the rates of molecular level processes from the analysis of macroscopic experimental measurements of the growth kinetics, in addition to the phenomenological parameters, such as lag times and maximal growth rates that are already obtainable from standard fitting procedures. We describe here an analytical approach based on fixed-point analysis, which provides self-consistent solutions for the growth of filamentous structures that can, in addition to elongation, undergo internal fracturing and monomer-dependent nucleation as mechanisms for generating new free ends acting as growth sites. Our results generalise the analytical expression for sigmoidal growth kinetics from the Oosawa theory for nucleated polymerisation to the case of fragmenting filaments. We determine the corresponding growth laws in closed form and derive from first principles a number of relationships which have been empirically established for the kinetics of the self-assembly of amyloid fibrils.

I Motivation and Historical Remarks

The characteristic aspects of filamentous growth processes, which involve assembly of elementary units to the ends of growing structures, have been investigated extensively over the past 50 years, with the physical concepts of nucleation and growth dating back a century further[1–7]. Contributing to this interest in the theory of filamentous growth phenomena is the realisation that such models have applications in polymer chemistry[8, 9] as well as close connections to biological phenomena such as the growth of biofilaments[10–14] including actin and tubulin, proteins involved in cytoskeletal structures, and the aberrant polymerisation of proteins associated with disease states such as sickle cell anemia[15], amyloid disorders[16–24] and the prion conditions[25–29].

Early investigations of filamentous growth[10, 11, 30] focused on homogeneous nucleation followed by linear polymerization. For irreversible growth in the absence of secondary

Europe PMC Funders Author Manuscripts

nucleation pathways, in 1962 Oosawa presented solutions to the kinetic equations which were very successful in describing a variety of characteristics of the polymerisation of actin and tubulin. In this framework of classical nucleated polymerisation, the mass concentration of polymer can be written as a simple closed form expression[10, 11, 31–33]:

$$M(t)=m_{\mathrm{tot}}\left[1-\mathrm{sech}^{2/n_c}\left(\sqrt{n_c/2}\lambda t\right)\right] \quad (1)$$

where $\lambda=\sqrt{2k_nk_+m_{\mathrm{tot}}^{n_c}}$ with k_n the nucleation rate constant, k_+ the elongation rate constant, n_c the critical nucleus size and m_{tot} is the total concentration of elementary units capable of polymerisation, hereafter referred to as monomers. This functional form describes a sigmoidal curve which is defined by the microscopic rate constants k_n and k_+. The aim of the present paper is to generalise Eq. (1) to include fragmenting of filaments and monomer-dependent secondary nucleation pathways.

A sigmoidal rate profile is characteristic of a wide class of *in vitro* protein assembly phenomena, including the growth of actin and tubulin[10–14, 34], and also amyloid fibrils formed by a variety of different proteins[16–18, 35]; it reflects the greater ease of aggregation of a monomer onto the ends of existing aggregate structures compared to *de novo* formation of a new aggregate from monomers alone through primary nucleation. The overall reaction rate, therefore, accelerates as significant numbers of aggregate structures are present in solution. Conversely, when much of the monomer population is incorporated into the aggregates, the reaction rate slows down due to the decrease in the availability of free monomers, and the sigmoidal profile reaches its plateau phase characteristic of the end-point of the reaction.

Detailed studies of actin polymerisation in the 1980s showed[36–38] that the mass concentration of polymers in a solution frequently is observed to increase more rapidly than the quadratic time dependence predicted by the Oosawa theory, Eq. (1), $M(t) \sim t^2$ for $t \rightarrow 0$, suggesting the extension of this model[36, 38, 39] to include secondary nucleation pathways, which can contribute to the increase in the number of polymers in addition to that produced by the straightforward homogeneous nucleation. More specifically, monomer-dependent secondary nucleation has been shown by Eaton and coworkers[15, 39, 40] to be of crucial importance for the formation of sickle hemoglobin fibers[39–44]. In addition, monomer-independent secondary nucleation in the form of fragmentation emerged as a key factor in the propagation of yeast[45–48] and mammalian prions[26, 49–53] and the growth of amyloid fibrils [35, 45, 46, 54, 55]. Except for special cases, however, general analytical treatments analogous to Eq. (1) of the classical nucleated growth problem in the presence of fragmentation or secondary nucleation have been challenging to achieve. Progress has instead been made with numerical solutions[37, 44, 56, 57] or perturbative treatments for early times in the reaction profile[36, 58]. Here we derive analytical results for the full polymerisation timecourse analogous to Eq. (1) for the case when secondary nucleation pathways, in particular filament breakage, are present. Building on our earlier work[59], we present a detailed analysis of this growth problem over a three part series. In the first part,

the general framework for obtaining self-consistent solutions to the growth problem is derived. In the second part, we discuss the accuracy of these solutions and present higher order expressions which yield scaling behaviour in close agreement with exact numerical results. In the final part we analyse the equilibrium behaviour of filamentous systems in the limit of long time scales.

II Master Equation and Principal Moments

The general strategy for deriving analytical results to the growth problem that generalises the Oosawa theory to include secondary pathways follows that of the original treatment[10]. The microscopic processes, as shown in Fig. 1, are described through a master equation; the principal moments, which are related to experimental observables, are obtained by summation of both sides of the master equation, resulting in a differential equation system for the evolution of the moments. These moment equations are non-linear and are not readily integrable; to address this challenge, in section III we obtain self-consistent solutions through the use of linearized solutions in an iterative fixed-point scheme.

The basic nucleation-elongation-fragmentation kinetics of an ensemble of polymers is governed by the master equation[10, 51, 54, 56, 60–63] for the time evolution of the concentrations $f(t, j)$ of chains of length j:

$$\begin{aligned}\frac{\partial f(t,j)}{\partial t} &= 2m(t)k_+ f(t,j-1) - 2m(t)k_+ f(t,j) + 2k_{\text{off}} f(t,j+1) - 2k_{\text{off}} f(t,j) \\ &\quad - k_-(j-1)f(t,j) \\ &\quad + 2k_- \sum_{i=j+1}^{\infty} f(t,i) + k_2 m(t)^{n_2} \sum_{i=n_c}^{\infty} i f(t,i)\delta_{j,n_2} + k_n m(t)^{n_c}\delta_{j,n_c}\end{aligned} \tag{2}$$

$$\frac{dm(t)}{dt} = -\frac{d}{dt}\left[\sum_{j=n_c}^{\infty} j \cdot f(t,j)\right] \tag{3}$$

where the time evolution of the free monomer concentration, $m(t)$, results from accounting for the monomer consumed through growth. The part of the equation pertaining to elongation (Fig. 1 b), $\partial_t^{\text{elong}} f(t,j) = 2m(t)k_+ f(t,j-1) - 2m(t)k_+ f(t,j)$, is that of Oosawa[10, 11] except for the factor of 2 which denotes growth from both ends[**?**]. The following two terms describe the possibility of depolymerisation from either end (Fig. 1 c)

to yield a polymer consisting of one less monomer[10, 11]. The breakage related term[37] $\partial_t^{\mathrm{frag}} f(t,j) = 2k_- \sum_{i=j+1}^{\infty} f(t,i)$ is responsible for the creation of smaller fragments when a longer filament breaks (Fig. 1 d). Since in this formulation breakage operates also for the bonds connecting the terminal monomers to the fibrils, it contributes to the effective depolymerisation rate which is given by $k_{\mathrm{off}} + k_-$. We note that in our treatment we neglect the association of filament fragments (the inverse process of breakage) in front of the other contributions; this process is important for simple polymers such as poly(methylstyrene) and for micelles[65–67], and has been proposed for the self-assembly of glutamate dehydrogenase[68]. For many protein polymers, including amyloid fibrils, detailed structural constraints are likely to prevent fusion of filaments unless they align both spatially and in terms of their respective orientations. It is observed experimentally that fragmentation dominates over association, thereby leading to a net increase in filament ends captured by a filament breakage rate[45, 46]. Lateral association of filaments, however, has been shown to occur[69, 70], and can result in a lower effective fragmentation rate. The second breakage related term $-k_-(j-1)f(t,j)$ accounts for decrease in the concentration of filaments of length j through the breakage of one of the $j-1$ internal bonds[51, 54, 56, 60–63]. The condition $f(t,j) = 0$ is imposed for all $j < n_c$, where $n_c \geq 2$ is the critical nucleus size for the filament growth; that is, all chains shorter than n_c are unstable. The concentration of monomers in the system is $m(t)$, and the last term in Eq. (2) represents the spontaneous formation of a growth nucleus of size $j = n_c$. The presence of a surface from pre-existing filaments can modify the nucleation barrier to forming aggregates from soluble monomer; this process is taken into account in the penultimate term in Eq. (2). The rate of this monomer-dependent secondary nucleation process[15, 39, 41, 58] is taken to be proportional to the total polymer concentration, and is governed by a rate constant k_2. For generality, the critical nucleus size for this process (Fig. 1 e), n_2, can be different to that of the primary nucleation process (Fig. 1 a).

Analytical approaches to tackle Eq. (2) can be directed towards the master equation itself, an approach that is discussed in [86], or the analysis of the principal moments of the distribution $f(t,j)$. The first two moments, the filament number $P(t)$ and mass $M(t)$ concentrations, constitute the most important experimentally accessible observables in such a filamentous system[10, 14, 39, 58, 71]. Higher order moments contain information on the shape of the filament length distribution. We focus on the polymer number and mass concentrations in Section A and outline a strategy to access information on the higher moments in Section B. In order to recover the full length distribution exactly, all higher moments are required. We show, however, in this paper and the second part of this series[86] that already the analysis of the first three moments provides a good approximation to the full distribution.

A Closed equation system for polymer number and mass concentrations

The kinetic equations for the first two moments, the number and mass concentrations

$$P(t) = \sum_j f(t,j) \tag{4}$$

$$M(t)=\sum_j j \cdot f(t,j) \quad (5)$$

can be found by taking the sum over j from n_c to ∞ on both sides of Eq. (2)[10, 14].

$$\frac{dP}{dt}=k_-[M(t)-(2n_c-1)P(t)]+k_2 m(t)^{n_2} M(t)+k_n m(t)^{n_c} \quad (6)$$

where the contribution ~ k_{off} $f(t, n_c)$ to the growth kinetics due to the destruction of fibrils through depolymerisation, k_{off}, has been neglected[36] in front of the creation of new seeds through primary and secondary nucleation.

The equation governing the dynamics of $M(t)$ can be found similarly and reads[10, 14, 51, 62, 72]:

$$\frac{dM}{dt}=2[m(t)k_+-k_{\text{off}}-k_- n_c(n_c-1)/2]P(t)+n_2 k_2 m(t)^{n_2} M(t)+n_c k_n m(t)^{n_c} \quad (7)$$

In summary, much of the dynamics of the system can be described in terms of the two principal moments, as the coupled non-linear differential equations (6) and (7). These equations make intuitive sense, e.g. the number of polymers at a given time, $P(t)$ in eq. (6), can increase if out of $M - P$ total bonds, the chains break at a location corresponding to more than $(n_c - 1)$ bonds from each end, thus accounting for the $[M - (2n_c - 1)P]$ factor. Similarly, the factor $n_c(n_c - 1)/2$ in the second moment equation (7) accounts for the fact that j monomers are created if a fibril fractures at an end closer than the critical nucleus size n_c, and therefore the total rate of monomers liberated through this mechanism from the ends of fibrils is $2k_-\sum_{j=1}^{n_c-1} jP$.

Many similar moment equations with analogous forms have been put forward in the context of different growth processes[10, 39, 45, 54, 56, 58, 60–63, 73]. The history of moment equations analogous to Eq. (7), which represents the starting point of our analysis in this section, can be traced back at least to the text book by Oosawa[10] in 1975, where they appear as equations (45), (46) and (58). The sigmoidal solution to the growth kinetics can be derived readily when k_- and k_2 are set to zero[10]. For the general case, which includes secondary nucleation, however, these equations are not readily integrable, but we show in the following sections that self-consistent solutions to this kinetic problem can be constructed in closed form.

B Equation systems for higher moments

The equations for the time evolution of the higher moments can be obtained using a similar approach to that used for $P(t)$ and $M(t)$. For these higher moments, however, each equation is coupled to that of a higher moment. A closed equation system for all moments ≤ n can be

Europe PMC Funders Author Manuscripts

obtained by neglecting the contribution from the central moment $\mu_{n+1}=\sum_{j=n_c}^{\infty}[j-M(t)/P(t)]^{n+1}/\sum_{j=n_c}^{\infty}P(t)$ to the coupled system. This procedure is illustrated here for the second, $Q(t)$, and third, $R(t)$, moments:

$$Q(t)=\sum_j j^2\cdot f(t,j) \qquad R(t)=\sum_j j^3\cdot f(t,j) \tag{8}$$

We note that whilst the zeroeth and first moments provide information on the mean fibril length, $L(t)$, these higher moments are related to higher central moments, the variance $V(t)$ and the skewness $S(t)$ of the fibril length distribution:

$$L(t)=\frac{M(t)}{P(t)} \tag{9}$$

$$V(t)=\frac{Q(t)}{P(t)}-\frac{M(t)^2}{P(t)^2} \tag{10}$$

$$S(t)=\frac{R(t)}{P(t)}-3\frac{M(t)Q(t)}{P(t)^2}+2\frac{M(t)^3}{P(t)^3} \tag{11}$$

We sketch out here the case for a fragmenting filament system where the contribution from the depolymerisation rate is negligible in front of that from the elongation rate. The time evolution of the second moment $Q(t)$ can be obtained from the master equation as:

$$\frac{dQ}{dt}=\sum_{j=n_c}^{\infty}2m(t)k_+j^2[f(t,j-1)-f(t,j)]-\sum_{j=n_c}^{\infty}k_-j^2(j-1)f(t,j)+2k_-\sum_{j=n_c}^{\infty}j^2\sum_{i=j+1}^{\infty}f(t,i)+\sum_{j=n_c}^{\infty}j^2k_nm^{n_c}\delta_{j,n_c} \tag{12}$$

Denoting the four sums as $A_1 \ldots A_4$ we note that the presence of the delta function in the fourth sum results in $A_4=n_c^2k_nm(t)^{n_c}$. The first sum simplifies to $\sum_j j^2[f(t,j-1)-f(t,j)] = \sum_j(2j+1)f(t,j)$, and therefore $A_1 = 2m(t)k_+[2M(t) + P(t)]$. Exchanging the order of summation in A_3 yields:

$$A_4=2k_-\sum_{j=n_c}^{\infty} j\sum_{i=j+1}^{\infty} f(t,i)=2k_-\sum_{i=n_c+1}^{\infty} f(t,i)\sum_{j=n_c}^{i-1} j^2=\frac{k_-}{3}\sum_{i=n_{c+1}}^{\infty} f(t,i)(i-n_c)(1-3i+2i^2-3n_c+2in_c+2n_c^2)$$

(13)

So that finally after reshuffling indices:

$$\frac{dQ}{dt}=2m(t)k_+[2M(t)+P(t)]+\frac{1}{3}k_-[M(t)+P(t)(3n_c^2-2n_c^3-n_c)-R(t)]+n_c^2k_nm(t)^{n_c} \quad (14)$$

This equation is not closed since it depends on the third moment $R(t)$, the time evolution of which in turn depends on a higher moment still. In order to obtain a closed equation system, we neglect the contribution to $Q(t)$ originating from the skewness of the filament length distribution. To this effect, we use Eq. (11) to substitute for the third moment in terms of the lower moments:

$$R(t)\approx 3\frac{M(t)Q(t)}{P(t)}-2\frac{M(t)^3}{P(t)^2} \quad (15)$$

Using this expression in Eq. (14) yields:

$$\frac{dQ}{dt}=2m(t)k_+[2M(t)+P(t)]+\frac{1}{3}k_-\left[M(t)+P(t)(3n_c^2-2n_c^3-n_c)-3\frac{M(t)Q(t)}{P(t)}+2\frac{M(t)^3}{P(t)^2}\right]+n_c^2k_nm(t)^{n_c}$$

(16)

which, together with Eq. (6) and (7) forms a closed system of equations.

III Self-Consistent Solutions for Frangible Filaments

We focus in the first part of this paper on systems where the dominant secondary process is filament fragmentation (Fig. 1 d); monomer-dependent secondary nucleation (Fig. 1 e) is considered in section IX. The underlying idea for solving Eqs. (6), (7) comes from the use of fixed-point iterations. This approach allows self-consistent solutions with increasing accuracy to be derived in an iterative process. In order to transform the differential equation system into a fixed-point problem, we integrate both sides of Eqs. (6), (7) with $k_2 = 0$ to yield:

$$\begin{pmatrix} P(t) \\ M(t) \end{pmatrix} = \begin{pmatrix} k_- \int_0^t e^{-(2n_c-1)k_-(t-\tau)} M(\tau) d\tau + P(0) e^{-(2n_c-1)k_- t} \\ M(\infty) \left(1 - \left(1 - \frac{M(0)}{M(\infty)} \right) e^{-2k_+ \int_0^t P(\tau) d\tau} \right) \end{pmatrix} \quad (17)$$

where $M(\infty) = [2k_+ m_{\text{tot}} - 2k_{\text{off}} - n_c(n_c - 1)k_-]/(2k_+)$ and we have neglected terms $\mathcal{O}(k_n)$ describing primary nucleation.

For $M(t)$ this approximation is accurate for all times, whereas for $P(t)$ it becomes increasingly accurate as the relative importance of primary nucleation to fragmentation in producing new fibrils decreases as the monomer is depleted. We use this operator to extend the validity of solutions which are exact in the early time limit, and in particular contain explicitly the contribution from primary nucleation proportional to k_n.

Let $\mathscr{A}$ denote the operator on the right-hand side of Eq. (17), such that Eq. (17) reads $\vec{x}(t) = \mathscr{A}[\vec{x}(t)]$ for $\vec{x}(t) = [P(t), M(t)]$. By construction, the fixed points $\vec{x}^*$ of $\mathscr{A}$:

$$\mathscr{A}[\vec{x}^*(t)] = \vec{x}^*(t) \quad (18)$$

are precisely the solutions to Eq. (17) for given initial conditions. According to the contraction mapping principle[74, 75] Eq. (18) can be solved iteratively:

$$\vec{x}^*(t) = \lim_{N \to \infty} \mathscr{A}^N [\vec{x}_0(t)] \quad (19)$$

for a starting value $\vec{x}_0(t)$ sufficiently close to $\vec{x}^*(t)$. The iteration therefore requires a good choice of starting value $\vec{x}_0(t)$; here the early stage solution to Eq. (6) is used. Even for small N in Eq. (19), the use of starting values $\vec{x}_0(t)$ that are exact for early times, in combination with the operator $\mathscr{A}$ that fixes exactly the late time behaviour, ensures that the result will interpolate between these exact limits and that the characteristic sigmoidal growth kinetics will be recovered.

IV Solutions to the Linearized Problem

A Number and mass concentration

As the starting value in the fixed-point scheme Eq. (18), we will use the well-known linear solutions[39, 58, 62, 63, 72] that emerge when the concentration of monomer is taken to be constant in time. This situation emerges either when the protein concentration is kept constant through the action of other mechanisms such as protein synthesis, or in the early time limit when $m(t) = m_{\text{tot}} - M(t) \approx m_{\text{tot}} - M(0) = m(0)$. In order to make explicit the approximations that will subsequently be taken, we write out these solutions in full below. In this limit, Eq. (6) becomes a linear differential equation system which can be solved by elementary methods:

Europe PMC Funders Author Manuscripts

$$\frac{dP_0(t)}{dt}=k_-[M_0(t)-(2n_c-1)P_0(t)]+k_n m(0)^{n_c} \quad (20)$$

$$\frac{dM_0(t)}{dt}=2[m(0)k_+ - k_{\text{off}} - k_- n_c(n_c-1)/2]P_0(t)+n_c k_n m(0)^{n_c} \quad (21)$$

to yield:

$$P_0(t)=C_1 e^{\kappa_1 t}+C_2 e^{\kappa_2 t} - \frac{\eta_2}{\xi_2} \quad (22)$$

where the constants are combinations of the rate constants: $\xi_1 = 2n_c - 1$, $\eta_1 = k_n m(0)^{n_c}$, $\xi_2 = 2m(0)k_+ - 2k_{\text{off}} - k_- n_c(n_c - 1)$ and $\eta_2 = n_c k_n m(0)^{n_c}$. The kinetic constants $\kappa_{1,2}$ are the roots of a quadratic equation:

$$\kappa_{1,2}=\frac{1}{2}\left(-k_-\xi_1 \pm \sqrt{k_-^2\xi_1^2+4k_-\xi_2}\right) \quad (23)$$

and the first moment $M_0(t)$ can then be solved to yield:

$$M_0(t)=\frac{C_1\xi_2}{\kappa_1}e^{\kappa_1 t}+\frac{C_2\xi_2}{\kappa_2}e^{\kappa_2 t} - \frac{\eta_1}{k_-} - \frac{\xi_1\eta_2}{\xi_2} \quad (24)$$

The coefficients $C_{1,2}$ are defined by the initial conditions $M(0)$ and $P(0)$:

$$C_{1,2}=\frac{1}{1-\frac{\kappa_{2,1}}{\kappa_{1,2}}}\left(\frac{\eta_2}{\xi_2} - \frac{\eta_1\kappa_{2,1}}{k_-\xi_2} - \frac{\xi_1\eta_2\kappa_{2,1}}{\xi_2^2}+P(0) - M(0)\frac{\kappa_{2,1}}{\xi_2}\right) \quad (25)$$

For most cases of practical interest $m(0)k_+ \gg k_-$; this condition guarantees the existence of a polymer population. The depolymerisation rate k_{off} is in general also very small compared to $k_+ m(0)$[36, 58] but can become comparable to this later quantity without fully compromising the existence of growing fibrils. Therefore we set $\xi_2 \approx 2[m(0)k_+ - k_{\text{off}}]$ and obtain:

$$\kappa = \pm\kappa_{1,2} \approx \pm\sqrt{2[m(0)k_+ - k_{\text{off}}]k_-} \quad (26)$$

Europe PMC Funders Author Manuscripts

$$P_0(t)=C_1e^{\kappa t}+C_2e^{-\kappa t}-\frac{n_c k_n m(0)^{n_c}}{2[m(0)k_+-k_{\text{off}}]} \quad (27)$$

$$M_0(t)=\frac{2[m(0)k_+-k_{\text{off}}]C_1}{\kappa}e^{\kappa t}-\frac{2[m(0)k_+-k_{\text{off}}]C_2}{\kappa}e^{-\kappa t}-\frac{k_n m(0)^{n_c}}{k_-} \quad (28)$$

with the constants C_1 and C_2 becoming:

$$C_{1,2}=\frac{P(0)}{2}\pm\frac{\kappa M(0)}{4[m(0)k_+-k_{\text{off}}]}+\frac{n_c k_n m(0)^{n_c}}{4[m(0)k_+-k_{\text{off}}]}\pm\frac{\kappa k_n m(0)^{n_c}}{4[m(0)k_+-k_{\text{off}}]k_-}\approx\frac{1}{2}\left(P(0)\pm\frac{\kappa M(0)}{2[m(0)k_+-k_{\text{off}}]}\pm\frac{\kappa k_n m(0)^{n_c}}{2[m(0)k_+-k_{\text{off}}]k_-}\right) \quad (29)$$

whereby the approximation in Eq. (29) originates from $\kappa \gg k_-$, which is equivalent to $m(0)k_+ \gg k_-$.

We note that in general the first term in the definition of $C_{1,2}$ is larger than the second one; indeed, equality is only reached when the condition $P(0)\kappa = M(0)k_-$ is satisfied. This condition cannot be met for stable seed structures since $M(0)k_-$ gives the increase in the number of polymers simply through the fragmentation of the seed structures and $P(0)\kappa$ is the initial slope of the exponential increase $P \sim P(0)e^{\kappa t}$ in the number of polymers from the growth process. Hence, if the condition $P(0)\kappa \ll M(0)k_-$ holds, the seed structures are not stable on the time scale of the growth process.

B Higher order moments

We can also derive solutions to the linearised problem that describes the time evolution of the higher moments. For simplicity, we consider here the case of a system which is initially in purely monomeric form, $Q(0) = M(0) = P(0) = 0$. The linearised solutions for $M(t)$ and $P(t)$, Eqs. (27) and (28), then read:

$$P(t)=\frac{\kappa C_+}{2k_+}\left(e^{\kappa t}-e^{-\kappa t}\right)=\frac{\kappa C_+}{k_+}sinh(\kappa t) \quad (30)$$

$$M(t)=m_{\text{tot}}C_+\left(e^{\kappa t}-e^{-\kappa t}\right)=2m_{\text{tot}}C_+cosh(\kappa t) \quad (31)$$

After substitution of the linearised solutions for $M(t)$ and $P(t)$ into Eq. (16) it is possible to solve for the second moment using the Ansatz:

$$Q(t)=\sum_{i=-\infty}^{\infty}\frac{(a_i+b_i t)e^{i\kappa t}}{(1+e^{\kappa t})^2} \quad (32)$$

with constants a_i and b_i. Substitution of the Ansatz into Eq. (16) yields the exact solution:

$$Q(t)=\frac{k_n m_{\mathrm{tot}}^{n_c-1}}{2k_-}\frac{e^{-\kappa t}}{(1+e^{\kappa t})^2}\left[\frac{m_{\mathrm{tot}}}{2}-\frac{4\kappa m_{\mathrm{tot}}}{3k_-}-\frac{\kappa}{12k_+}-\frac{k_- n_c}{12k_+}+\frac{k_- n_c^2}{4k_+}-\frac{k_- n_c^3}{6k_+}+e^{\kappa t}\left(2m_{\mathrm{tot}}+\frac{8\kappa m_{\mathrm{tot}}}{3k_-}-\frac{k_- n_c}{3k_+}-\frac{\kappa n_c^2}{k_+}+\frac{k_- n_c^2}{k_+}-\frac{2k_-}{3k_+}\right.\right.$$

(33)

This result may be simplified by keeping only leading order terms under the inequality $k_+ m_{\mathrm{tot}} \gg k_-$, implying also $\kappa \gg k_-$[59]:

$$Q(t)\approx\frac{64C_+k_+m_{\mathrm{tot}}^{n_c+1}}{3\kappa}\mathrm{cosech}(\kappa t)sinh\left(\frac{\kappa t}{2}\right)^4 \quad (34)$$

Comparison with Eqs. (30) and (31) further reveals that there is a simple connection between the three first moments in the linear regime:

$$Q(t)=\frac{4}{3}\frac{M(t)^2}{P(t)} \quad (35)$$

This result is valid for times $t \gg (k_+ m_{\mathrm{tot}})^{-1}$, corresponding to all but extremely early times in the polymerisation reaction, which occurs over a time-scale $\kappa^{-1} \gg (k_+ m_{\mathrm{tot}})^{-1}$. The accuracy of the result Eq. (34) compared to the full numerical result which accounts for the third central moment is shown in Fig. 3.

V Solution to the Non-Linear Moment Equations

The full time course of the polymerisation reaction can now be solved iteratively from Eq. (19) by applying the operator $\mathscr{A}$ to the early time solution in Eqs. (28) and (27):

$$\begin{pmatrix} P_N(t) \\ M_N(t) \end{pmatrix}=\mathscr{A}^N\left[\begin{pmatrix} P_0(t) \\ M_0(t) \end{pmatrix}\right] \quad (36)$$

The first order expression $N=1$ for $M(t)$ follows then from substituting Eq. (27) into (17):

$$M(t)=M(\infty)\left[1-\left(1-\frac{M(0)}{M(\infty)}\right)exp\left(-2k_+\int_0^t C_1e^{\kappa\tau}+C_2e^{-\kappa\tau}-\frac{n_ck_nm(0)^{n_c}}{2[m(0)k_+-k_{\text{off}}]}d\tau\right)\right]$$

(37)

For most cases of practical interest, $M(0) \ll M(\infty)$ allowing the approximation $1 - M(0)/M(\infty) \approx \exp(-M(0)/M(\infty))$. On integration, Eq. (37) then yields:

$$M(t)=M(\infty)\left[1-exp\left(-C_+e^{\kappa t}+C_-e^{-\kappa t}+\frac{k_+n_ck_nm(0)^{n_c}}{m(0)k_+-k_{\text{off}}}t+D\right)\right] \quad (38)$$

Generally the breakage rate is small in the sense that for the duration of the experiment, $t<k_-^{-1}$ (i.e. most individual bonds in the system do not fracture over the time course of the reaction) and therefore Eq. (38) can be simplified to:

$$M(t)=M(\infty)\left[1-exp\left(-C_+e^{\kappa t}+C_-e^{-\kappa t}+D\right)\right] \quad (39)$$

with $C_\pm = C_{1,2}2k_+/\kappa$ and $D=\frac{\lambda_0^2}{\kappa^2}-M(0)/M(\infty)+\frac{k_+M(0)}{m(0)k_+-k_{\text{off}}}$. Using the approximation in Eq. (40) corresponding to the case $k_- \ll \kappa$, similarly to Eq. (29), finally yields:

$$C_\pm=\frac{k_+P(0)}{\kappa}\pm\frac{M(0)k_+}{2[m(0)k_+-k_{\text{off}}]}\pm\frac{\lambda_0^2}{2\kappa^2} \quad (40)$$

where $\lambda_0=\sqrt{2k_nk_+m(0)^{n_c}}$ is the effective rate constant derived by Oosawa[10, 11] for nucleated polymerisation without secondary pathways, Eq. (1) and Appendix. The expression Eq. (39) describes in closed form the time evolution of systems characterised by nucleated polymerisation and fragmentation.

The shape described by this function is somewhat similar to that of the logistic function $M(t) = m_{\text{tot}}/[1 + e^{m_{\text{tot}}kt}m(0)/M(0)]$ which emerges as a solution of simple autocatalytic reactions: $m \rightarrow M$, $dM(t)/dt = kM(t)m(t)$ with rate constant k. Logistic functions and generalised logistic functions (Richards' functions) have been successfully used to fit[76–85] the growth kinetics of protein aggregation as they describe sigmoidal curves. The rate constants in the logistic function and in related sigmoidal curves do not, however, in general have an interpretation as microscopic rate constants when applied to the more complex case of filamentous growth, as the logistic modelling neglects the nature of the linear growth process as a polymerisation rather than a simple autocatalytical reaction.

VI Analysis of Limiting Cases

In this section a range of limiting cases of Eq. (39) that are of particular practical interest are highlighted. Neglecting terms that are not significant in specific limits allows in many cases more compact forms to be given for the integrated rate laws.

A Early time limit

For early times when $t \ll \kappa^{-1}$ and $M(t)/M(\infty) \ll 1$ we can expand the outer exponential in Eq. (39) yield:

$$M(t) \approx M(\infty)C_+e^{\kappa t} - M(\infty)C_-e^{-\kappa t} - DM(\infty) \quad (41)$$

$$\approx m(0)[C_+e^{\kappa t} - C_-e^{-\kappa t}] - \frac{k_n m(0)^{n_c}}{k_-} = M_0(t) \quad (42)$$

This functional form recovers the exponential behaviour characteristic of situations with constant monomer concentration[58].

B Long time limit

The expression Eq. (39) can be simplified for long times $t \gg \kappa^{-1}$, as the argument of the first exponential will be dominated by the increasing exponential term $e^{\kappa t}$ in the sum, and therefore in this regime the linear, constant and exponentially decaying terms can be neglected yielding:

$$M(t) = M(\infty)[1 - exp(-C_+e^{\kappa t})] \qquad t \gg \kappa^{-1} \quad (43)$$

a form which has the advantage of possessing an exact closed form integral function, contrary to the full expression Eq. (39), a fact which can be exploited in deriving higher order results[86].

C Irreversible filament growth

In the absence of depolymerisation, $k_{off} = 0$, and for cases of small or no initial seed material, $m(0) \approx m_{tot}$, Eq. (39) reduces to:

$$M(t) = m_{tot}\left[1 - exp\left(-C_+e^{\kappa t} + C_-e^{-\kappa t} + \frac{\lambda_0^2}{\kappa^2}\right)\right] \quad (44)$$

where

$$C_{\pm} \approx \frac{k_+ P(0)}{\kappa} \pm \frac{M(0)}{2m_{\mathrm{tot}}} \pm \frac{\lambda_0^2}{2\kappa^2} \quad (45)$$

since $M(\infty) \approx m(0) \approx m_{\mathrm{tot}}$ and so $D \approx \lambda_0^2/\kappa^2$. The effect of varying the depolymerisation rate is shown in Fig. 5.

Interestingly, we note that in the case of irreversible growth, the time evolution of the polymer mass depends on three combinations of the kinetic parameters: k_+, λ_0 and κ, whereas in the case of irreversible growth without secondary pathways (Eq. (1) and Appendix), the kinetics depends primarily on k_+ and λ_0.

D Absence of seed material

When $M(0) = P(0) = 0$, implying $m(0) = m_{\mathrm{tot}}$, Eq. (39) can be compacted using the double angle formulae to yield:

$$M(t) = M(\infty)\left[1 - exp\left(-4C_+ sinh^2\left(\frac{\kappa t}{2}\right)\right)\right] \quad (46)$$

with

$$C_+ = \frac{\lambda^2}{2\kappa^2} \quad (47)$$

where only one constant C_+ is required as in this limit $C_+ = -C_-$. In this case, the evolution of the polymer mass depends only upon two combinations of the rate constants, κ and λ. In comparison, the Oosawa theory for filament growth without secondary pathways, Eq. (1) and Appendix, shows that in the absence of seeds the kinetics then depend primarily only upon λ.

E Infrangible filaments

It is interesting to consider the limit of equation (38) where nucleation is more important in producing new ends than breakage, $k_- \to 0$; in this situation, the rate of production of new fibrils is independent of the quantity of existing fibrils, in contrast to the case where fragmentation is active. The limit $k_- \to 0$ implies $\kappa \to 0$, and therefore the inner exponentials can be expanded in series yielding up to quadratic order:

$$M(t) = M(\infty)\left\{1 - exp\left(-C_+\left[1 + \kappa t + \frac{\kappa^2 t^2}{2}\right] + C_-\left[1 - \kappa t + \frac{\kappa^2 t^2}{2}\right] + D + \frac{k_+ n_c k_n m(0)^{n_c}}{[m(0)k_+ - k_{\mathrm{off}}]} t\right)\right\}$$

(48)

The constants $C_{1,2}$ diverge as ~ κ^{-1}, implying that the pre-factors in Eq. (48) diverge only quadratically with κ and therefore terms in the expansion $\mathcal{O}(\kappa^3)$ and higher will tend to zero with $k_- \rightarrow 0$ resulting in:

$$M(t)=M(\infty)\left\{1-exp\left(-[C_+-C_-]-\kappa t\,[C_++C_-]-\frac{\kappa^2 t^2}{2}[C_+-C_-]+D+\frac{k_+ n_c k_n m(0)^{n_c}}{[m(0)k_+-k_{\text{off}}]}t\right)\right\} \quad (49)$$

Substituting the expressions for $C_\pm = C_{1,2}2k_+/\kappa$ from Eq. (29) and setting also the depolymerisation rate to zero as in[10, 11], Eq. (49) yields:

$$M(t)=m_{\text{tot}}\left[1-exp\left(-k_+k_n m_{\text{tot}}^{n_c}t^2-2k_+P(0)t-\frac{M(0)}{m_{\text{tot}}}\right)\right] \quad (50)$$

It is interesting to note that Eq. (50) is essentially equivalent to the Johnson-Mehl-Avrami-Kolmogorov (JMAK) equation, originally derived for crystallisation[6, 7]:

$$M(t)=m_{\text{tot}}\left[1-exp\left(Km_{\text{tot}}^{n_c}t^{d+1}\right)\right] \quad (51)$$

if one considers one-dimension, $d = 1$, and if we keep the leading order t^2 time dependency and identify k_+k_n with K. In one dimension the JMAK equation is analogous to the nucleated growth of polymers[87, 88], and therefore this equivalence is to be expected as we set $k_- = 0$.

The structure of the solution for early times can be analysed by expanding the remaining exponential function for small values of the exponent to yield:

$$M_0(t)=M(0)+k_+k_n m_{\text{tot}}^{n_c+1}t^2+2k_+m_{\text{tot}}P(0)t+n_ck_nm_{\text{tot}}^{n_c}t \quad (52)$$

Therefore, in the absence of breakage, when nucleation is the dominant process contributing to the creation of new ends, fibril growth tends to a polynomial form in time, and we recover the ~ t^2 dependence of the Oosawa solution Eq. (1).

In addition to the direct interaction of n_c monomers to form a critical nucleus[10, 58, 89], a variety of other schemes have been proposed in the literature for the primary nucleation term that lead to a zeroth and first moment in the form of a polynomial relationship[15, 32, 58, 71, 90–98], including pre-equilibrium and lattice-based models. For example, nucleation could occur via the rapid equilibrium of sub-critically sized small oligomers $f(t, j)+m \leftrightarrow f(t, j+1)$ with a single equilibrium constant K to form oligomers up to a critical size n_*. Upon monomer addition, such an oligomer transforms into aggregates capable of elongating from j

$= n_c$ to $j = \infty$ with a rate k_+, and this process can be captured with an overall nucleation rate $\partial_t^{\text{nucl}} f(t,j) = 2k_+ K m^{n_*} \sim m^{n_*+1}$.

As a further consistency check, it can be verified that the limiting case of Eq. (39), given by Eq. (52), is identical to the exact elementary solution of the linear differential equation system:

$$\frac{dP_0}{dt} = k_n m(0)^{n_c} \tag{53}$$

$$\frac{dM_0}{dt} = 2k_+ m(0) M_0 + n_c k_n m(0)^{n_c} \tag{54}$$

obtained as the zeroth and first moments of the length distribution $f(j, t)$ from the master equation Eq. (2) in the absence of breakage $k_- = 0$ and for constant monomer concentration $m = m(0)$.

VII Polymer Number Concentration

In order to evaluate the time evolution of the number of polymers $P(t)$, the second component of $\mathscr{A}(M_0, P_0)$ is required. To this effect the fixed point iteration Eq. (17) is carried out up to second order; this procedure effectively leads to substituting the result in Eq. (39) (first order) as a sub-expression in Eq. (17). Rearranging the terms and neglecting the linear and inverse exponential terms in front of the growing exponential yields:

$$P(t) = M(\infty) k_- e^{-(2n_c-1)k_- t} \left\{ \frac{P(0)}{k_- M(\infty)} + \frac{e^{(2n_c-1)k_- t} - 1}{(2n_c-1)k_-} - \int_0^t exp\left(-C_+ e^{\kappa t}\right) d\tau \right\} \tag{55}$$

and now the integral has a closed form expression in terms of the exponential integral function $Ei(t) = -\int_{-t}^{\infty} e^{-s}/s ds$:

$$P(t) = k_- M(\infty) e^{-(2n_c-1)k_- t} \left[\frac{P(0)}{k_- M(\infty)} + \frac{e^{(2n_c-1)k_- t} - 1}{(2n_c-1)k_-} - \frac{1}{\kappa} Ei\left(-C_+ e^{\kappa t}\right) + \frac{1}{\kappa} Ei\left(-C_+\right) \right] \tag{56}$$

which is exact for $t = 0$ and in the long time limit $t \gg \kappa^{-1}$.

VIII Analysis of the Central Moments

A Mean length

The mean length of the filament population is given by the ratio of the two first raw moments:

$$L(t)=\frac{M(t)}{P(t)} \quad (57)$$

At early times in the growth reaction, when the monomer concentration is approximately constant, this expression reads:

$$L_0(t)=\frac{M_0(t)}{P_0(t)}=\frac{\frac{2[m(0)k_+-k_{\text{off}}]C_1}{\kappa}e^{\kappa t}-\frac{2[m(0)k_+-k_{\text{off}}]C_2}{\kappa}e^{-\kappa t}-\frac{k_n m(0)^{n_c}}{k_-}}{C_1e^{\kappa t}+C_2e^{-\kappa t}-\frac{n_c k_n m(0)n_c}{2[m(0)k_+-k_{\text{off}}]}} \quad (58)$$

which in the absence of initial seed material takes the form of a hyperbolic tangent:

$$L_0(t)=\frac{2\left(k_+m(0)-k_{\text{off}}\right)}{\kappa}tanh\left(\kappa t\right) \quad (59)$$

For long times, these expressions approach the limit:

$$\lim_{t\to\infty}L_0(t)=\frac{2\left(k_+m(0)-k_{\text{off}}\right)}{\kappa} \quad (60)$$

and so, whilst in a system where the monomer concentration is held constant, the polymer number and polymer mass concentrations increase exponentially for large times, their ratio tends to a constant.

At later times, as the monomer is depleted, the full non-linear solutions for $M(t)$, Eq. (39), and $P(t)$, Eq. (56), show that the length decreases due to fragmentation dominating over elongation:

$$L(t)=\frac{M(t)}{P(t)}=\frac{e^{(2n_c-1)k_-t}\left[1-exp\left(-C_+e^{\kappa t}+C_-e^{-\kappa t}+D\right)\right]}{\frac{P(0)}{M(\infty)}+\frac{e^{(2n_c-1)k_-t}-1}{(2n_c-1)}-\frac{k_-}{\kappa}Ei\left(-C_+e^{\kappa t}\right)+\frac{k_-}{\kappa}Ei\left(-C_+\right)} \quad (61)$$

After the growth phase, which occurs over a timescale of order $1/\kappa$, the polymer mass remains approximately constant whereas the polymer number continues to increase over a timescale of $1/k_-$, as shown in Fig. (9), hence leading to a decrease in the average filament length. This functional form is illustrated in Fig. 10 A. The average length of fibrils formed has two phases: initially fibrils elongate and the average length increases and reaches a

maximum given approximately by the limit of the linearized solution, Eq. (60); subsequently, as the available monomer is depleted, fragmentation of the formed fibrils results in a reduction in their mean length.

B Standard deviation

The variance of the filament population is given in terms of the first three raw moments:

$$V(t)=\frac{Q(t)}{P(t)}-L(t)^2 \tag{62}$$

At early times in the growth reaction, when the monomer concentration is approximately constant, calculating the standard deviation of the distribution using Eq. (34) yields the compact result:

$$\begin{aligned}\sqrt{V(t)}&=\sqrt{\frac{Q(t)}{P(t)}-\frac{M(t)^2}{P(t)^2}}\\&=\frac{1}{\sqrt{3}}L(t)\end{aligned} \tag{63}$$

This result shows that for a system of fragmenting filaments growing in constant monomer concentration, the filament length distribution evolves such that the ratio of the mean filament length to the standard deviation of the distribution of filament lengths is constant.

As the monomer becomes depleted at the end of the reaction, the filament population shifts towards shorter lengths under the action of fragmentation; this process leads to the decrease of both the mean filament length and the standard deviation of the filament length distribution. The form of this decrease is closely analogous for both central moments; an observation that can be verified also in the limit:

$$\begin{aligned}\lim_{t\to\infty}\frac{\sqrt{V(t)}}{L(t)}&=\frac{1}{2\sqrt{3}}\sqrt{\frac{1-\frac{1}{n_c^2}}{\left(1-\frac{1}{2n_c}\right)^3}}\\&=\frac{1}{2\sqrt{3}}\left(1+\frac{3}{4n_c}+\mathcal{O}\left(n_c^{-2}\right)\right)\end{aligned} \tag{64}$$

In this limit for large times, therefore, the ratio of the standard deviation to the mean filament length differs by less than a factor of two relative to the ratio at early times, with the two limits being closer for small nucleus sizes. The ratio of the length and standard deviation remains a number of the order unity over the whole timecourse of the reaction; this fact can be used to evaluate the width of the distribution during late times as shown in Fig. 10 B.

IX Monomer Dependent Secondary Nucleation

We now illustrate the wider applicability of the fixed-point scheme to growth phenomena characterised by secondary nucleation pathways other than fragmentation. We take here the example of monomer-dependent secondary nucleation (Fig. 1 e), the analysis of which was

pionered by Eaton and coworkers for the polymerisation of sickle hemoglobin in the 1980s[40, 99]. In such a system the time evolution of the principal moments can be approximated as (cf. Eqs. (6) and (7) and Refs. [40, 99, 100]):

$$\frac{dP(t)}{dt}=k_2M(t)m(t)^{n_2}+k_nm(t)^{n_c} \quad (65)$$

$$\frac{dM(t)}{dt}=2\left(m(t)k_+ - k_{\text{off}}\right)P(t)+n_ck_nm(t)^{n_c}+n_2k_2M(t)m(t)^{n_2} \quad (66)$$

It is interesting to note that these differential equations go over to Eqs. (7) when direct production or consumption of monomers through secondary nucleation is neglected in front of the monomer consumption through filament elongation for the growth stages; for the $t\rightarrow\infty$ limit discussed in[101], these terms can however become important.

We sketch out the derivation in this paper of first order self-consistent solutions to this growth problem. These solutions are valid for longer times than the linear and perturbative expressions that were derived earlier[58]. Due to the highly non-linear nature of these differential equations, however, especially for $n_2 \gg 1$, their analysis is significantly more challenging than for the case discussed in the first part of this paper where fragmentation is the dominant secondary pathway. Therefore, we expect the firsr order self-consistent solutions derived below to be less accurate than the equivalent results for the case of fragmenting filaments. In the second part of this series[86] we present a detailed derivation and analysis of higher order solutions which are able to describe accurately the full time course of the reaction, even for values of n_c, $n_2 \gg 1$.

As for the case of frangible filaments, we begin with the linearized solutions to the equations (66) which read[58]:

$$P_0(t)=C_1e^{\kappa t}+C_2e^{-\kappa t}+\frac{\left(n_2-n_c\right)k_nm(0)^{n_c}}{2\left[m(0)k_+ - k_{\text{off}}\right]} \quad (67)$$

$$M_0(t)=\frac{2\left[m(0)k_+ - k_{\text{off}}\right]C_1}{\kappa}e^{\kappa t}-\frac{2\left[m(0)k_+ - k_{\text{off}}\right]C_2}{\kappa}e^{-\kappa t}-\frac{k_n}{k_2}m(0)^{n_c-n_2} \quad (68)$$

with the relevant constants:

$$\kappa=\sqrt{2m(0)^{n_2}\left[m(0)k_+ - k_{\text{off}}\right]k_2} \quad (69)$$

$$C_{\pm} \equiv C_{1,2} 2k_+/\kappa \quad (70)$$

$$= \frac{k_+ P(0)}{\kappa} \pm \frac{k_+ M(0)}{2\left[m(0)k_+ - k_{\text{off}}\right]} - \frac{(n_2 - n_c)\, k_+ k_n m(0)^{n_c}}{2\kappa\left[m(0)k_+ - k_{\text{off}}\right]} \pm \frac{k_n m(0)^{n_c - n_2}}{2\left[m(0)k_+ - k_{\text{off}}\right] k_2} \quad (71)$$

$$\approx \frac{k_+ P(0)}{\kappa} \pm \frac{k_+ M(0)}{2\left[m(0)k_+ - k_{\text{off}}\right]} \pm \frac{\lambda_0^2}{2\kappa^2} \quad (72)$$

for $\lambda_0 = \sqrt{2k_n k_+ m(0)^{n_c}}$, Eq. (1). The large majority of monomer consumed is from the term $2k_+m(t)P(t)$ (elongation of existing filaments) and the nucleation terms mainly contribute indirectly through the increase in $P(t)$; therefore we can formally solve the time evolution for $M(t)$ under the action of the term $2k_+m(t)P(t)$ to yield the second component of a fixed-point equation for $[P, M]$:

$$M(t) = M(\infty)\left[1 - exp\left(-\frac{M(0)}{M(\infty)} - 2k_+ \int_0^t P(\tau)d\tau\right)\right] \quad (73)$$

for $M(\infty) \approx m_{\text{tot}} - \frac{k_{0\text{ff}}}{k_+}$, which emerges from Eq. (66) under the action of the dominant monomer consumption through its incorporation into fibrils and neglecting direct monomer consumption from the nucleation processes. The first iteration yields the first order self-consistent solution for the polymer mass concentration $M(t)$:

$$M_1(t) \approx M(\infty)\left[1 - exp\left(-C_+ e^{\kappa t} + C_- e^{-\kappa t} + D\right)\right] \quad (74)$$

where $D = \frac{\lambda_0^2}{\kappa^2} - M(0)/M(\infty) + \frac{k_+ M(0)}{m(0)k_+ - k_{\text{off}}}$. Due to the action of the fixed point operator, the validity of this solution is extended in time when compared to the linearized equations which form the starting point of this analysis.

X Discussion of the Characteristics of Fibrillar Growth

Important characteristics of nucleated elongation and fragmentation kinetics are briefly discussed in this section based on Eq. (39) which predicts, as a function of time, the changes in the number of monomers that are incorporated into polymers.

A Maximal growth rate

The analytical form Eq. (43) for the growth kinetics can be used to investigate the dependence of the maximal growth rate $r_{\max}$ on different parameters:

$$r_{\max}=\left[\frac{dM(t)}{dt}\right]_{t=t_{\max}}=M(\infty)\kappa C_{+}e^{\kappa t_{\max}}e^{-C_{+}e^{\kappa t_{\max}}} \quad (75)$$

where $t_{\max}$ is the solution of:

$$\begin{aligned}0&=\left[\frac{d^{2}M(t)}{dt^{2}}\right]_{t=t_{\max}}\\&=M(\infty)\kappa C_{+}(\kappa-\kappa C_{+}e^{\kappa t_{\max}})e^{\kappa t_{\max}}e^{-C_{+}e^{kt_{\max}}}\end{aligned} \quad (76)$$

yielding:

$$t_{\max}=\frac{\log(1/C_{+})}{\kappa} \quad (77)$$

and

$$r_{\max}=\frac{M(\infty)\kappa}{e} \quad (78)$$

Interestingly Eq. (78) is independent of C_{+} and therefore of the initial conditions. In other words, the maximal rate of the reaction depends only on the kinetic parameters k_{+}, k_{-} and the total protein concentration, but not on the number of polymers present initially in the solution or the nucleation rate k_{n}. This universality breaks down for conditions where the lag phase disappears completely (equivalent to $C_{+}+C_{-}>C_{c}$), as discussed in section X B. The time, given by Eq. (77), at which the reaction reaches the maximal rate is on the other hand dependent on the details of the system.

B Lag phase and convex rate profile

Eq. (77) has the interesting feature that the initial rate of growth $\dot{M}(0)=r_{0}<r_{\max}$ is smaller than the maximal rate of growth $r_{\max}$ in many cases, implying the presence of a lag phase. This effect can be analysed in more detail: since $r_{0}=m_{\text{tot}}\kappa(C_{+}+C_{-})$, the condition $r_{0}<r_{\max}$ is equivalent to:

$$C_{+}+C_{-}<C_{c}=\frac{1}{e} \quad (79)$$

Or substituting for $C_{+}+C_{-}$ from Eq. (29):

$$\frac{2k_+P(0)}{\kappa}+\frac{k_+n_ck_nm(0)^{n_c}}{\kappa[m(0)k_+-k_{\text{off}}]}<\frac{1}{e} \quad (80)$$

This observation naturally suggest a definition for a critical seed-concentration $M_c = P_cL_0$ assuming the fibrils have an initial length of L_0 as:

$$M_c=\frac{\kappa L_0}{2k_+e} \quad (81)$$

or a critical nucleation rate k_n^c :

$$k_n^c=\frac{\kappa[m(0)k_+-k_{\text{off}}]}{k_+n_ck_nm(0)^{n_c}e} \quad (82)$$

above which the lag phase ceases to exist, and the polymerisation rate is fastest initially and then decays as the free monomer in solution is being used up. This result can be compared with the rate profiles shown in Fig. 11; the conditions used result in a critical seed-concentration of $M_c = 260\ \mu$M, and all curves with $M < M_c$ indeed exhibit a lag phase.

In particular, these results demonstrate that the length of the lag phase does not necessarily correspond to the time required to form the initial growth nuclei, as has sometimes been assumed. In fact, a lag phase can exist even when seed fibrils are present at $t = 0$ and no primary nucleation occurs.

C Lag time and correlation with growth rate

A key characteristic of filamentous growth is the commonly observed presence of a lag phase prior to the conversion of the majority of soluble material into filamentous structures. Two commonly used definitions of this lag time are discussed. First, an arbitrary concentration threshold m_{th} can be defined; this concentration could, for example, correspond to an experimental threshold above which the presence of polymer can be detected. The time to reach this value will be $\tau_{\text{lag}} = 1/\kappa \log(m_{\text{th}}/m_{\text{tot}} \cdot 1/C_+)$ if we assume that the threshold value is small $m_{\text{th}} \ll m_{\text{tot}}$. Note that the length of this lag phase scales inversely with the kinetic parameter κ. The other frequently used way to measure the lag phase is to extrapolate the maximal growth rate back to zero polymer concentration, and use the intersection with the time axis as the value for the lag phase as shown in Fig. 4. Let us evaluate this quantity from the model for polymerisation driven by secondary pathways: the rate of maximal growth occurs from Eq. (77) at $t_{\text{max}} = \log(1/C_+)/\kappa$ and for the concentration $m_r = M(\infty)(1 - e^{-1})$. The condition $m_r/(t_{\text{max}} - \tau_{\text{lag}}) = r_{\text{max}}$ implies that the lag time has the form:

$$\tau_{\text{lag}}=[\log(1/C_+)-e+1]\kappa^{-1} \quad (83)$$

Europe PMC Funders Author Manuscripts

again inversely proportional to κ. In particular, in both cases, the lag time follows approximately a power law with respect to the initial monomer concentration, $\tau_{\mathrm{lag}} \sim m(0)^{\gamma}$, with an exponent of $\gamma = -(n_2 + 1)/2$ since $\kappa \sim m(0)^{-(n_2+1)/2}$ when monomer-dependent secondary nucleation is dominant and $\gamma = -1/2$ when fragmentation dominates ($n_2 = 0$). This scaling is analogous to that predicted by Oosawa[10] for primary nucleated systems $\tau_{\mathrm{lag}} \sim m(0)^{-n_c/2}$. Nucleation in general necessitates a molecular collision, $n_c \geq 2$, and therefore a sub-extensive scaling of the lag time with monomer concentration is indicative of fragmentation, rather than nucleation dominated growth.

More generally, as the kinetic equations for nucleated polymerisation and for the growth of breakable filaments are given in the form of sigmoidal equations that principally depend on a specific combination of the individual rate parameters (either κ for growth dominated by secondary processes, or λ for growth dominated by primary nucleation), these factors will also dominate the values of the macroscopic observables that characterise the growth process. In particular we find a correlation between the lag phase and the maximal growth rate which emerges as a consequence of this observation. Indeed, for filaments growing under the action of secondary pathways, the maximal growth rate r_{max} scales with κ, and hence there must very generally exist an inverse correlation between the lag phase τ_{lag} and the maximal growth rate r_{max} as the specific initial conditions enter only logarithmically through $\log(1/C_+)$.

This strong correlation has been empirically established for a variety of amyloid fibrils systems[102–104]. The results discussed above show that it is not necessary to assume a correlation between the elongation and nucleation rates to observe such an effect. Instead, the present analysis shows that this connection between growth rate and duration of the lag phase is inherent to the way that both observables are strongly influenced by the same kinetic parameter.

XI Conclusion

Self-consistent solutions to the sigmoidal growth kinetics of fragmenting structures have been derived, and the accuracy of the solutions relative to numerical data has been verified. In contrast to linearized solutions which are valid only for early times, the self-consistent solutions discussed in this paper remain accurate for the full time course of the polymerization reaction. Due to the applicability of such self-consistent solutions over the full duration of the reaction, we recover the characteristic sigmoidal behaviour observed for protein aggregation experiments. Our results, therefore, represent a theoretical framework for analyzing experimental observations of filamentous growth in terms of microscopic rate constants, rather than the phenomenological parameters available heretofore from fitting data to empirical sigmoid functions. We have also shown that in the limit of vanishing breakage rate our analysis replicates the well-known results for nucleated growth given by the Oosawa theory. Our results furthermore provide a unified explanation from first principles for a wide range of empirically established relationships for amyloid growth.

Appendix

We examine briefly the behaviour of the Oosawa solutions[10] to the kinetics of irreversible nucleated polymerisation without depolymerisation or secondary pathways. For a system that evolves through primary nucleation of new filaments and elongation of existing filaments, the change in concentration of filaments of size *j*, denoted *f*(*j*, *t*), is given by the master equation[10, 11]:

$$\frac{\partial f(t,j)}{\partial t}=2m(t)k_+f(t,j-1)-2m(t)k_+f(t,j)+k_nm(t)^{n_c}\delta_{j,n_c} \quad (84)$$

From Eq. (84), the rate of change of the number of filaments, *P*(*t*), and the free monomer concentration, *m*(*t*), were shown by Oosawa[10, 11] to approximately obey:

$$\frac{dP}{dt}=k_nm(t)^{n_c} \quad (85)$$

$$\frac{dm}{dt}=-2k_+m(t)P(t) \quad (86)$$

Combining Eqs. (85) and (86) yields a differential equation for the free monomer concentration[10]:

$$-\frac{d^2}{dt^2}\log(m(t))=2k_+k_nm(t)^{n_c} \quad (87)$$

for which Oosawa stated the solution in the case of all the protein being soluble at $t = 0$ (i.e. no added seed)[10], Eq.(1). Here, we sketch out briefly the general solution, which includes a finite concentration of seed material present at the start of the reaction. Performing the substitution $z(t) := \log(m(t))$ and multiplying through by dz/dt:

$$-\frac{d}{dt}\left[\frac{n_c}{4k_+k_n}\left(\frac{dz}{dt}\right)^2\right]=\frac{d}{dt}e^{n_cz} \quad (88)$$

Integrating both sides:

$$-\frac{n}{2}\left(\frac{dz}{dt}\right)^2=2k_+k_ne^{n_cz}+A=-\frac{d^2z}{dt^2}+A \quad (89)$$

we obtain a separable equation for dz/dt, which can be solved to yield:

$$\frac{dz}{dt}=\sqrt{\frac{2A}{n_c}}\tanh\left(\frac{\sqrt{2An_c}}{2}(-t+2B)\right) \quad (90)$$

Integration and exponentiation yields the expression for $m(t)$:

$$m(t)=\left[\frac{A}{2k_+k_n}\operatorname{sech}\left(\sqrt{\frac{An_c}{2}}(t-2B)\right)^2\right]^{1/n_c} \quad (91)$$

Inserting the appropriate boundary conditions in terms of $m(0)$ and $P(0)$ fixes the values of the constants A and B, resulting in the final exact result for the polymer mass concentration $M(t) = m_{\text{tot}} - m(t)$:

$$M(t)=m_{\text{tot}}-m(0)\left[\mu\operatorname{sech}\left(\nu+\lambda_0\beta^{-\frac{1}{2}}\mu t\right)\right]^{\beta} \quad (92)$$

where the effective rate constant λ_0 is given by $\lambda_0=\sqrt{2k_nk_+m(0)^{n_c}}$ and $\beta = 2/n_c$, $\mu=\sqrt{1+\gamma}$, $\nu = \operatorname{arsinh}(\gamma)$ for $\gamma=P(0)k_+n_c/(\beta^{-\frac{1}{2}}\lambda_0)$.

In the special case of the aggregation reaction starting with purely soluble proteins, $P(0) = 0$, $m(0) = m_{\text{tot}}$, these expressions reduce to $\lambda_0 \rightarrow \lambda$, $\mu \rightarrow 1$ and $\nu \rightarrow 0$, and Eq. (92) yields the result presented by Oosawa[10], Eq. (1).

In many cases, Eq. (92) describes a sigmoid with a lag phase. The time of maximal growth rate, t_{max}, can be found from the inflection point of the sigmoid from the condition $d^2M/dt^2 = 0$:

$$t_{\max}=\left[\operatorname{artanh}\left(\sqrt{\frac{1}{1+\beta}}\right)-\operatorname{arsinh}(\gamma)\right](\mu\beta^{-\frac{1}{2}}\lambda_0)^{-1} \quad (93)$$

such that a lag phase only exists for:

$$\operatorname{artanh}\left(\sqrt{\frac{1}{1+\beta}}\right)>\operatorname{arsinh}(\gamma) \quad (94)$$

which is equivalent to the requirement:

$$P(0)\sqrt{\frac{2k_+}{k_nm(0)^{n_c}}}<1 \quad (95)$$

Europe PMC Funders Author Manuscripts

and so an increased nucleation rate promotes the existence of an inflection point, whereas an increased elongation rate or an increased level of seeding tends to disfavour its existence. In particular, we also note that in the absence of nucleation, an inflection point cannot exist.

The corresponding maximal growth rate, r_{max}, is given by:

$$r_{max}=\frac{2m(0)}{\sqrt{n_c(2+n_c)}}\left(\frac{2\mu^2}{2+n_c}\right)^{\frac{1}{n_c}}\mu\beta^{-\frac{1}{2}}\lambda_0 \quad (96)$$

which occurs at:

$$M(t_{max})=m_{\mathrm{tot}}-m(0)\mu^{\frac{2}{n_c}}\left(1-\frac{n_c^2}{(2+n_c)^2}\right)^{\frac{1}{n_c}} \quad (97)$$

The lag time, $\tau_{\mathrm{lag}} := t_{\max} - M(t_{\max})/r_{\max}$, is then given by:

$$\tau_{\mathrm{lag}}=\left[\operatorname{artanh}\left(\sqrt{\frac{1}{1+\beta}}\right)-\operatorname{arsinh}(\gamma)-\frac{m_{\mathrm{tot}}-m(0)\mu^{\frac{2}{n_c}}\left(1-\frac{n_c^2}{(2+n_c)^2}\right)^{\frac{1}{n_c}}}{\frac{2m(0)}{\sqrt{n_c(2+n_c)}}\left(\frac{2\mu^2}{2+n_c}\right)^{\frac{1}{n_c}}}\right]\left(\mu\beta^{-\frac{1}{2}}\lambda_0\right)^{-1} \quad (98)$$

Additionally, an expression for the evolution of the polymer number concentration, $P(t)$ may be derived. Using Eq. (92), direct integration of Eq. (85) gives the result for $P(t)$:

$$P(t)=P(0)+k_n m(0)^{n_c}\mu\frac{tanh(\nu+\beta^{-\frac{1}{2}}\lambda_0\mu t)-tanh(\nu)}{\beta^{-\frac{1}{2}}\lambda_0} \quad (99)$$

and we note that a point of inflection can never exist for $P(t)$.

References

[1]. Gibbs JW. On the equilibrium of heterogeneous substances. Trans Conn Acad Arts Sci. 1878; 3:108, 343.

[2]. Volmer M, Weber A. Keimbildung in übersättigten Gebilden. Z Phys Chem. 1926; 119:277.

[3]. Kaischew R, Stranski IN. The theory of the linear rate of crystallisation. Z phys Chem. 1934; A170:295.

[4]. Stranski IN, Kaischew R. Crystal growth and crystal nucleation. Z Phys. 1935; 36:393.

[5]. Becker R, Döring W. Kinetische Behandlung der Keimbildung in übersättigten Dämpfen. Ann Phys. 1935; 26:719. 5.

[6]. Avrami M. Kinetics of Phase Change. I. General Theory. J Chem Phys. 1939; 7(12):1103.

[7]. Avrami M. Kinetics of Phase Change. II. Transformation-Time Relations for Random Distribution of Nuclei. J Chem Phys. 1940; 8(2):212.

[8]. Flory, P. Principles of Polymer Chemistry. Cornell University Press; 1953.

[9]. Flory, P. Statistical Mechanics of Chain Molecules. Interscience; 1969.

[10]. Oosawa, F.; Asakura, S. Thermodynamics of the Polymerization of Protein. Academic Press; 1975.

[11]. Oosawa F, Kasai M. A theory of linear and helical aggregations of macromolecules. J Mol Biol. 1962; 4:10. [PubMed: 14482095]

[12]. Tobacman LS, Korn ED. The kinetics of actin nucleation and polymerization. J Biol Chem. 1983; 258:3207. [PubMed: 6826559]

[13]. Frieden C, Goddette DW. Polymerization of actin and actin-like systems: evaluation of the time course of polymerization in relation to the mechanism. Biochemistry. 1983; 22:5836. [PubMed: 6661414]

[14]. Wegner A, Engel J. Kinetics of the cooperative association of actin to actin filaments. Biophys Chem. 1975; 3:215. [PubMed: 1174645]

[15]. Hofrichter J, Ross PD, Eaton WA. Kinetics and mechanism of deoxyhemoglobin S gelation: a new approach to understanding sickle cell disease. Proc Natl Acad Sci U S A. 1974; 71:4864. [PubMed: 4531026]

[16]. Dobson CM. Protein misfolding, evolution and disease. Trends Biochem Sci. 1999; 24:329. [PubMed: 10470028]

[17]. Chiti F, Dobson CM. Protein misfolding, functional amyloid, and human disease. Annu Rev Biochem. 2006; 75:333. [PubMed: 16756495]

[18]. Dobson CM. Protein folding and misfolding. Nature. 2003; 426:884. [PubMed: 14685248]

[19]. Cohen FE, Kelly JW. Therapeutic approaches to protein-misfolding diseases. Nature. 2003; 426:905. [PubMed: 14685252]

[20]. Selkoe DJ. Folding proteins in fatal ways. Nature. 2003; 426:900. [PubMed: 14685251]

[21]. Lansbury PT, Lashuel HA. A century-old debate on protein aggregation and neurodegeneration enters the clinic. Nature. 2006; 443:774. [PubMed: 17051203]

[22]. Pepys MB. Pathogenesis, diagnosis and treatment of systemic amyloidosis. Phil Trans R Soc Lond B. 2001; 356:203. [PubMed: 11260801]

[23]. Hardy J, Selkoe DJ. The amyloid hypothesis of Alzheimer's disease: progress and problems on the road to therapeutics. Science. 2002; 297:353. [PubMed: 12130773]

[24]. Sacchettini JC, Kelly JW. Therapeutic strategies for human amyloid diseases. Nat Rev Drug Discov. 2002; 1:267. [PubMed: 12120278]

[25]. Prusiner SB. Molecular biology of prion diseases. Science. 1991; 252:1515. [PubMed: 1675487]

[26]. Come JH, Fraser PE, Lansbury PT. A kinetic model for amyloid formation in the prion diseases: importance of seeding. Proc Natl Acad Sci U S A. 1993; 90:5959. [PubMed: 8327467]

[27]. Aguzzi A, Haass C. Games played by rogue proteins in prion disorders and Alzheimer's disease. Science. 2003; 302:814. [PubMed: 14593165]

[28]. Falsig J, Nilsson KP, Knowles TPJ, Aguzzi A. Chemical and biophysical insights into the propagation of prion strains. HFSP J. 2008; 2:332. [PubMed: 19436493]

[29]. Aguzzi A, O'Connor T. Protein aggregation diseases: pathogenicity and therapeutic perspectives. Nat Rev Drug Discov. 2010; 9:237. [PubMed: 20190788]

[30]. Oosawa F, Asakura S, Hotta K, Imai N, Ooi T. G-F transformation of actin as a fibrous condensation. J Poly Sci. 1959; 37:323.

[31]. Ataka M. Nucleation and growth kinetics of hen egg-white lysozyme crystals. Prog Crystal Growth and Charact. 1995; 30:109.

[32]. Flyvbjerg H, Jobs E, Leibler S. Kinetics of self-assembling microtubules: an "inverse problem" in biochemistry. Proc Natl Acad Sci U S A. 1996; 93:5975. [PubMed: 8650204]

[33]. Powers ET, Powers DL. The kinetics of nucleated polymerizations at high concentrations: amyloid fibril formation near and above the "supercritical concentration". Biophys J. 2006; 91:122. [PubMed: 16603497]

[34]. Cooper JA, Buhle EL, Walker SB, Tsong TY, Pollard TD. Kinetic evidence for a monomer activation step in actin polymerization. Biochemistry. 1983; 22:2193. [PubMed: 6860660]

[35]. Knowles TPJ, Oppenheim TW, Buell AK, Chirgadze DY, Welland ME. Nanostructured films from hierarchical self-assembly of amyloidogenic proteins. Nat Nanotechnol. 2010; 5:204. [PubMed: 20190750]

[36]. Bishop MF, Ferrone FA. Kinetics of nucleation-controlled polymerization. A perturbation treatment for use with a secondary pathway. Biophys J. 1984; 46:631. [PubMed: 6498276]

[37]. Wegner A. Kinetic analysis of actin assembly suggests that tropomyosin inhibits spontaneous fragmentation of actin filaments. J Mol Biol. 1982; 161:217. [PubMed: 7154079]

[38]. Wegner A. Spontaneous fragmentation of actin filaments in physiological conditions. Nature. 1982; 296:266. [PubMed: 7199623]

[39]. Ferrone FA, Hofrichter J, Eaton WA. Kinetics of sickle hemoglobin polymerization. II. A double nucleation mechanism. J Mol Biol. 1985; 183:611. [PubMed: 4020873]

[40]. Ferrone FA, Hofrichter J, Sunshine HR, Eaton WA. Kinetic studies on photolysis-induced gelation of sickle cell hemoglobin suggest a new mechanism. Biophys J. 1980; 32:361. [PubMed: 7248455]

[41]. Ferrone FA, Hofrichter J, Eaton WA. Kinetics of sickle hemoglobin polymerization. I. Studies using temperature-jump and laser photolysis techniques. J Mol Biol. 1985; 183:591. [PubMed: 4020872]

[42]. Ferrone FA, Ivanova M, Jasuja R. Heterogeneous nucleation and crowding in sickle hemoglobin: an analytic approach. Biophys J. 2002; 82:399. [PubMed: 11751326]

[43]. Hofrichter J. Kinetics of sickle hemoglobin polymerization. III. Nucleation rates determined from stochastic fluctuations in polymerization progress curves. J Mol Biol. 1986; 189:553. [PubMed: 3783684]

[44]. Medkour T, Ferrone F, Galactros F, Hannaert P. The double nucleation model for sickle cell haemoglobin polymerization: full integration and comparison with experimental data. Acta Biotheor. 2008; 56:103. [PubMed: 18247134]

[45]. Collins SR, Douglass A, Vale RD, Weissman JS. Mechanism of prion propagation: amyloid growth occurs by monomer addition. PLoS Biol. 2004; 2:e321. [PubMed: 15383837]

[46]. Tanaka M, Collins SR, Toyama BH, Weissman JS. The physical basis of how prion conformations determine strain phenotypes. Nature. 2006; 442:585. [PubMed: 16810177]

[47]. Perrett S, Jones GW. Insights into the mechanism of prion propagation. Curr Opin Struct Biol. 2008; 18:52. [PubMed: 18243685]

[48]. Chernoff YO, Lindquist SL, Ono B, Inge-Vechtomov SG, Liebman SW. Role of the chaperone protein Hsp104 in propagation of the yeast prion-like factor [psi+]. Science. 1995; 268:880. [PubMed: 7754373]

[49]. Jarrett JT, Lansbury PT. Seeding ”one-dimensional crystallization” of amyloid: a pathogenic mechanism in Alzheimer’s disease and scrapie? Cell. 1993; 73:1055. [PubMed: 8513491]

[50]. Harper JD, Lieber CM, Lansbury PT. Atomic force microscopic imaging of seeded fibril formation and fibril branching by the Alzheimer’s disease amyloid-beta protein. Chem Biol. 1997; 4:951. [PubMed: 9427660]

[51]. Nowak MA, Krakauer DC, Klug A, May RM. Prion Infection Dynamics. Integrative Biology. 1998; 1:3.

[52]. Collinge J, Clarke AR. A general model of prion strains and their pathogenicity. Science. 2007; 318:930. [PubMed: 17991853]

[53]. Baskakov IV. Branched chain mechanism of polymerization and ultrastructure of prion protein amyloid fibrils. FEBS J. 2007; 274:3756. [PubMed: 17617227]

[54]. Hall D, Edskes H. Silent prions lying in wait: a two-hit model of prion/amyloid formation and infection. J Mol Biol. 2004; 336:775. [PubMed: 15095987]

[55]. Xue W-F, Hellewell AL, Gosal WS, Homans SW, Hewitt EW, Radford SE. Fibril fragmentation enhances amyloid cytotoxicity. J Biol Chem. 2009; 284:34272. [PubMed: 19808677]

[56]. Xue W-F, Homans SW, Radford SE. Systematic analysis of nucleation-dependent polymerization reveals new insights into the mechanism of amyloid self-assembly. Proc Natl Acad Sci U S A. 2008; 105:8926. [PubMed: 18579777]

[57]. Wright CF, Teichmann SA, Clarke J, Dobson CM. The importance of sequence diversity in the aggregation and evolution of proteins. Nature. 2005; 438:878. [PubMed: 16341018]

[58]. Ferrone F. Analysis of protein aggregation kinetics. Methods Enzymol. 1999; 309:256. [PubMed: 10507029]

[59]. Knowles TPJ, Waudby CA, Devlin GL, Cohen SIA, Aguzzi A, Vendruscolo M, Terentjev EM, Welland ME, Dobson CM. An analytical solution to the kinetics of breakable filament assembly. Science. 2009; 326:1533. [PubMed: 20007899]

[60]. Carulla N, Caddy GL, Hall DR, Zurdo J, Gair M, Feliz M, Giralt E, Robinson CV, Dobson CM. Molecular recycling within amyloid fibrils. Nature. 2005; 436:554. [PubMed: 16049488]

[61]. Pallitto MM, Murphy RM. A mathematical model of the kinetics of beta-amyloid fibril growth from the denatured state. Biophys J. 2001; 81:1805. [PubMed: 11509390]

[62]. Poeschel T, Brilliantov NV, Froemmel C. Kinetics of prion growth. Biophys J. 2003; 85:3460. [PubMed: 14645042]

[63]. Kunes KC, Cox DL, Singh RRP. One-dimensional model of yeast prion aggregation. Phys Rev E Stat Nonlin Soft Matter Phys. 2005; 72:051915. [PubMed: 16383653]

[64]. There is evidence in the literature for both unidirectional[105] and bidirectional[106] growth of amyloid fibrils. Detailed studies[107, 108] suggest that growth is likely in general to be bidirectional but with a varying degree of polarity implying that in most cases one end of the fibril grows much faster than the other. These considerations do not affect the steady state growth kinetics of fibrils, and in all cases we can identify $2k_+m(t)f(t, j)$ with a total rate of length increase.

[65]. Cates ME. Nonlinear viscoelasticity of wormlike micelles (and other reversibly breakable polymers). J Phys Chem. 1990; 94:371.

[66]. Granek R, Cates ME. Stress relaxation in living polymers: Results from a Poisson renewal model. J Chem Phys. 1992; 96:4758.

[67]. Maestro A, Acharya DP, Furukawa H, Gutirrez JM, Arturo L-QM, Ishitobi M, Kunieda H. Formation and disruption of viscoelastic wormlike micellar networks in the mixed surfactant systems of sucrose alkanoate and polyoxyethylene alkyl ether. J Phys Chem B. 2004; 108:14009.

[68]. Thusius D, Dessen P, Jallon JM. Mechanisms of bovine liver glutamate dehydrogenase self-association. I. Kinetic evidence for a random association of polymer chains. J Mol Biol. 1975; 92:413. [PubMed: 1142429]

[69]. Ionescu-Zanetti C, Khurana R, Gillespie JR, Petrick JS, Trabachino LC, Minert LJ, Carter SA, Fink AL. Monitoring the assembly of Ig light-chain amyloid fibrils by atomic force microscopy. Proc Natl Acad Sci U S A. 1999; 96:13175. [PubMed: 10557293]

[70]. Khurana R, Ionescu-Zanetti C, Pope M, Li J, Nielson L, Ramrez-Alvarado M, Regan L, Fink AL, Carter SA. A general model for amyloid fibril assembly based on morphological studies using atomic force microscopy. Biophys J. 2003; 85:1135. [PubMed: 12885658]

[71]. Lomakin A, Teplow DB, Kirschner DA, Benedek GB. Kinetic theory of fibrillogenesis of amyloid beta-protein. Proc Natl Acad Sci U S A. 1997; 94:7942. [PubMed: 9223292]

[72]. Masel J, Jansen VA, Nowak MA. Quantifying the kinetic parameters of prion replication. Biophys Chem. 1999; 77:139. [PubMed: 10326247]

[73]. Smith JF, Knowles TPJ, Dobson CM, Macphee CE, Welland ME. Characterization of the nanoscale properties of individual amyloid fibrils. Proc Natl Acad Sci U S A. 2006; 103:15806. [PubMed: 17038504]

[74]. Zeidler, E. Nonlinear Functional Analysis and its Applications: Part 1: Fixed-Point Theorems. Springer; 1985.

[75]. Granas, A.; Dugundji, J. Fixed Point Theory. Springer-Verlag; 2003.

[76]. Nielsen L, Khurana R, Coats A, Frokjaer S, Brange J, Vyas S, Uversky VN, Fink AL. Effect of environmental factors on the kinetics of insulin fibril formation: elucidation of the molecular mechanism. Biochemistry. 2001; 40:6036. [PubMed: 11352739]

[77]. Padrick SB, Miranker AD. Islet amyloid: phase partitioning and secondary nucleation are central to the mechanism of fibrillogenesis. Biochemistry. 2002; 41:4694. [PubMed: 11926832]

[78]. Hamada D, Dobson CM. A kinetic study of beta-lactoglobulin amyloid fibril formation promoted by urea. Protein Sci. 2002; 11:2417. [PubMed: 12237463]

[79]. Sabat R, Gallardo M, Estelrich J. An autocatalytic reaction as a model for the kinetics of the aggregation of beta-amyloid. Biopolymers. 2003; 71:190. [PubMed: 12767118]

[80]. Librizzi F, Rischel C. The kinetic behavior of insulin fibrillation is determined by heterogeneous nucleation pathways. Protein Sci. 2005; 14:3129. [PubMed: 16322584]

[81]. Lee C-C, Nayak A, Sethuraman A, Belfort G, McRae GJ. A three-stage kinetic model of amyloid fibrillation. Biophys J. 2007; 92:3448. [PubMed: 17325005]

[82]. Watzky MA, Morris AM, Ross ED, Finke RG. Fitting yeast and mammalian prion aggregation kinetic data with the Finke-Watzky two-step model of nucleation and autocatalytic growth. Biochemistry. 2008; 47:10790. [PubMed: 18785757]

[83]. Morris AM, Watzky MA, Finke RG. Protein aggregation kinetics, mechanism, and curve-fitting: a review of the literature. Biochim Biophys Acta. 2009; 1794:375. [PubMed: 19071235]

[84]. Morris AM, Watzky MA, Agar JN, Finke RG. Fitting neurological protein aggregation kinetic data via a 2-step, minimal/"Ockham's razor" model: the Finke-Watzky mechanism of nucleation followed by autocatalytic surface growth. Biochemistry. 2008; 47:2413. [PubMed: 18247636]

[85]. Morris AM, Finke RG. Alpha-synuclein aggregation variable temperature and variable pH kinetic data: a re-analysis using the Finke-Watzky 2-step model of nucleation and autocatalytic growth. Biophys Chem. 2009; 140:9. [PubMed: 19101068]

[86]. Cohen SIA, Vendruscolo M, Dobson CM, Knowles TPJ. Nucleated polymerisation with secondary pathways II. Determination of self-consistent solutions to growth processes described by non-linear master equations. 2010 submitted.

[87]. Bromley EHC, et al. Assembly pathway of a designed alpha-helical protein fiber. Biophys J. 2010; 98:1668. [PubMed: 20409488]

[88]. Kashchiev D, Auer S. Nucleation of amyloid fibrils. J Chem Phys. 2010; 132:215101. [PubMed: 20528047]

[89]. Ferrone FA. Nucleation: the connections between equilibrium and kinetic behavior. Methods Enzymol. 2006; 412:285. [PubMed: 17046664]

[90]. Firestone SKRMP, De Levie R. On one-dimensional nucleation and growth of "living polymers". I. Homogeneous nucleation. J Theor Biol. 1983; 104:553. [PubMed: 6645561]

[91]. Goldstein RF, Stryer L. Cooperative polymerization reactions. Analytical approximations, numerical examples, and experimental strategy. Biophys J. 1986; 50:583. [PubMed: 3779001]

[92]. Ataka M, Ogawa T. Nucleation and growth of oxide precipitates in CZ-Si wafers. J Mater Res. 1993; 11:2889.

[93]. Bessho Y, Ataka M, Asai M, Katsura T. Analysis of the crystallization kintics of lysozyme using a model with polynuclear growth mechanism. Biophys J. 1994; 66:310. [PubMed: 8161684]

[94]. Murphy RM, Pallitto MM. Probing the kinetics of beta-amyloid self-association. J Struct Biol. 2000; 130:109. [PubMed: 10940219]

[95]. Chen S, Ferrone FA, Wetzel R. Huntington's disease age-of-onset linked to polyglutamine aggregation nucleation. Proc Natl Acad Sci U S A. 2002; 99:11884. [PubMed: 12186976]

[96]. Wetzel R. Kinetics and thermodynamics of amyloid fibril assembly. Acc Chem Res. 2006; 39:671. [PubMed: 16981684]

[97]. Andrews JM, Roberts CJ. A Lumry-Eyring nucleated polymerization model of protein aggregation kinetics: 1. Aggregation with pre-equilibrated unfolding. J Phys Chem B. 2007; 111:7897. [PubMed: 17571872]

[98]. Serio TR, Cashikar AG, Kowal AS, Sawicki GJ, Moslehi JJ, Serpell L, Arnsdorf MF, Lindquist SL. Nucleated conformational conversion and the replication of conformational information by a prion determinant. Science. 2000; 289:1317. [PubMed: 10958771]

[99]. Eaton WA, Hofrichter J. Proceedings of the Symposium on Clinical and Biochemical Aspects of Hemoglobin Abnormalities. 1978

[100]. Ruschak AM, Miranker AD. Fiber-dependent amyloid formation as catalysis of an existing reaction pathway. Proc Natl Acad Sci U S A. 2007; 104:12341. [PubMed: 17640888]

[101]. Cohen SIA, Vendruscolo M, Dobson CM, Knowles TPJ. Nucleated polymerisation with secondary pathways III. Equilibrium behaviour, filament length distribution and oliogomer populations. 2010 Submitted.

[102]. Klement K, Wieligmann K, Meinhardt J, Hortschansky P, Richter W, Fändrich M. Effect of different salt ions on the propensity of aggregation and on the structure of Alzheimer's abeta(1-40) amyloid fibrils. J Mol Biol. 2007; 373:1321. [PubMed: 17905305]

[103]. Fändrich M. Absolute correlation between lag time and growth rate in the spontaneous formation of several amyloid-like aggregates and fibrils. J Mol Biol. 2007; 365:1266. [PubMed: 17141269]

[104]. Meinhardt J, Tartaglia GG, Pawar A, Christopeit T, Hortschansky P, Schroeckh V, Dobson CM, Vendruscolo M, Fändrich M. Similarities in the thermodynamics and kinetics of aggregation of disease-related Abeta(1-40) peptides. Protein Sci. 2007; 16:1214. [PubMed: 17525469]

[105]. Ban T, Hoshino M, Takahashi S, Hamada D, Hasegawa K, Naiki H, Goto Y. Direct observation of Abeta amyloid fibril growth and inhibition. J Mol Biol. 2004; 344:757. [PubMed: 15533443]

[106]. Scheibel T, Kowal AS, Bloom JD, Lindquist SL. Bidirectional amyloid fiber growth for a yeast prion determinant. Curr Biol. 2001; 11:366. [PubMed: 11267875]

[107]. DePace AH, Weissman JS. Origins and kinetic consequences of diversity in Sup35 yeast prion fibers. Nat Struct Biol. 2002; 9:389. [PubMed: 11938354]

[108]. Inoue Y, Kishimoto A, Hirao J, Yoshida M, Taguchi H. Strong growth polarity of yeast prion fiber revealed by single fiber imaging. J Biol Chem. 2001; 276:35227. [PubMed: 11473105]

Europe PMC Funders Author Manuscripts

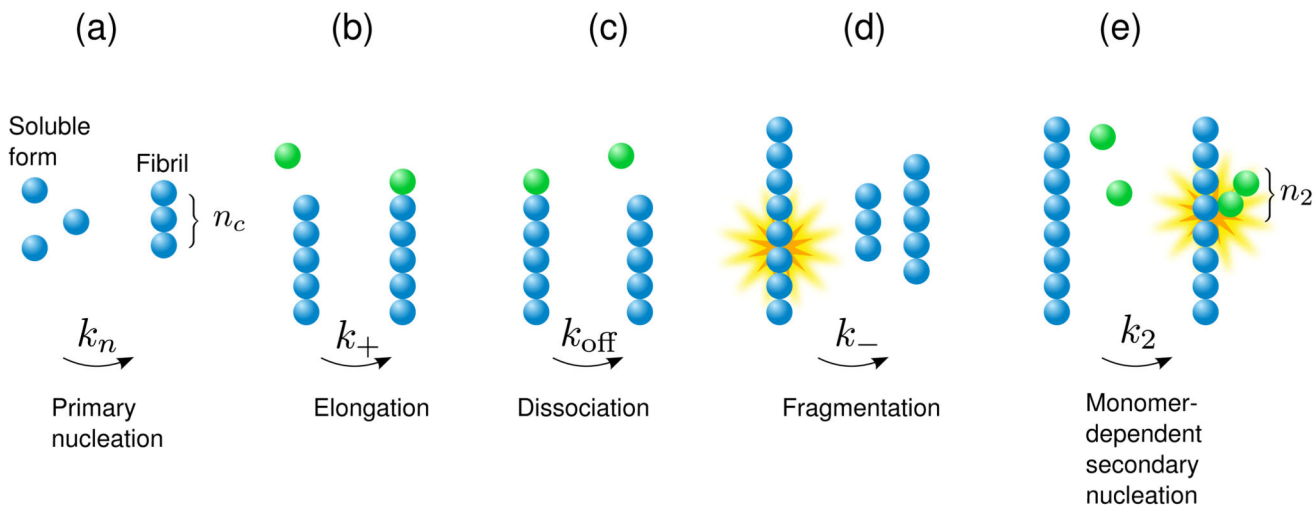

Fig. 1.

Schema illustrating the microscopic processes of polymerisation with secondary pathways treated in this paper. Primary nucleation (a) leads to the creation of a polymer of length n_c from soluble monomer. Filaments grow linearly (b) from both ends in a reversible manner with monomers also able to dissociate from the ends (c). The secondary pathways (d) and (e) lead to the creation of of new fibril ends from pre-existing polymers; fragmentation (d) is discussed in the first part of this paper, and monomer-dependent secondary nucleation (e) is discussed in the second part.

Europe PMC Funders Author Manuscripts

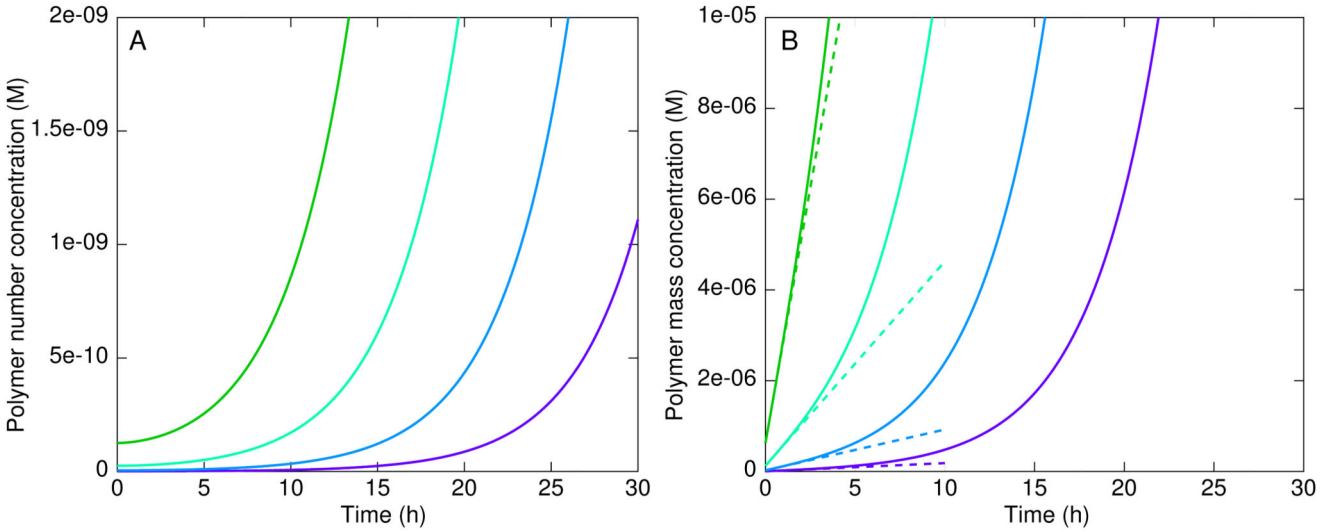

Fig. 2.

Growth kinetics in the early time limit with different initial seed concentrations (from left to right): $M(0) = 6.25 \cdot 10^{-7}$. $M(0) = 1.25 \cdot 10^{-7} M$, $M(0) = 2.5 \cdot 10^{-8} M$, $M(0) = 5 \cdot 10^{-9}$, The other parameters are: $k_{off} = 0$, $P(0) = M(0)/5000$, $k_+ = 5 \cdot 10^4\ M^{-1}\ s^{-1}$, $k_{off} = 0$, $k_- = 10^{-9}\ s^{-1}$ $k_n = 0$, $m_{tot} = 5 \cdot 10^{-5} M$. In (A) is $P(t)$ the zeroth moment of the distribution $f(t, j)$ given by Eq. (28) and in (B) is $M(t)$ the first moment from Eq. (27). The dashed lines in (B) show the initial rate $dM/dt|_{t=0} = 2k_+ m_{tot} P|_{t=0}$.

Europe PMC Funders Author Manuscripts

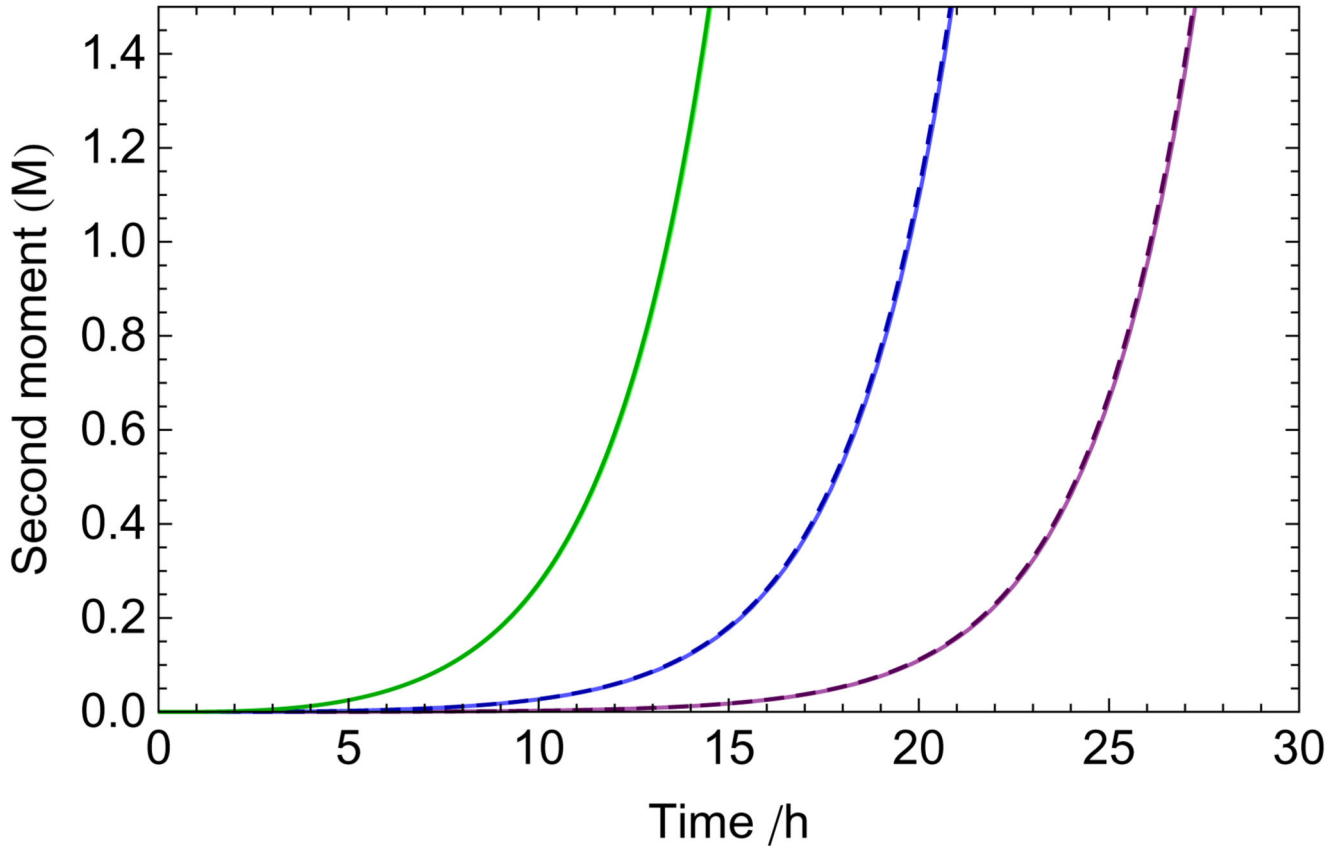

Fig. 3.

Time evolution of the second moment $Q(t)$ of the length distribution in the early time limit for differing primary nucleation rates (from left to right): $k_n = 2 \cdot 10^{-3}$ M^{-1} s^{-1}, $k_n = 2 \cdot 10^{-4}$ M^{-1} s^{-1}, $k_n = 2 \cdot 10^{-5}$ M^{-1} s^{-1}. The other parameters are: $k_+ = 5 \cdot 10^4$ M^{-1} s^{-1}, $k_{off} = 0$, $k_- = 2 \cdot 10^{-8}$ s^{-1}, $m_{tot} = 5 \cdot 10^{-6}$ M, $n_c = 2$, $M(0) = P(0) = 0$. The dashed lines show the analytical result Eq. (34) derived by neglecting the third central moment. The solid lines show the numerical result from the master equation, Eq. (2), which accounts for all central moments.

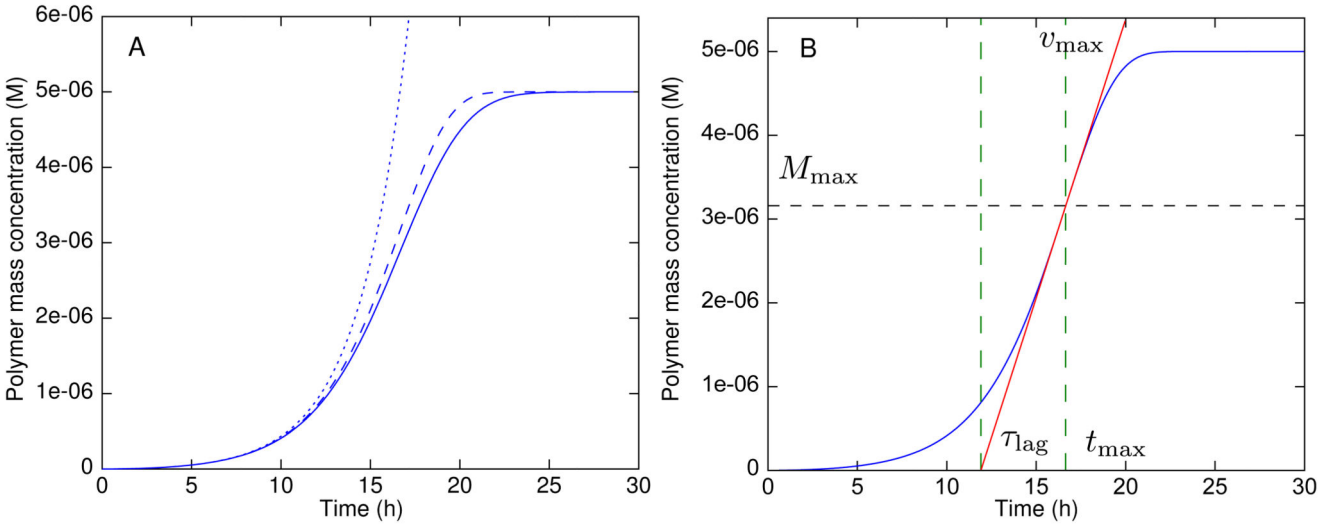

Fig. 4.

Kinetics of fibrillar growth. Growth through nucleation, elongation and fragmentation leads to sigmoidal kinetic curves for the mass concentration of fibrils as a function of time. Solid line: first moment $M(t)$ computed from the numerical solution of the master equation Eq. (2). Dashed curve: analytical solution given in Eq. (39). Dotted curve: early time limit from Eq. (28). The parameters are: $k_+ = 5 \cdot 10^4\ \mathrm{M}^{-1}\ \mathrm{s}^{-1}$, $k_{\mathrm{off}} = 0$, $k_- = 2 \cdot 10^{-8}\ \mathrm{s}^{-1}$, $m_{\mathrm{tot}} = 5 \cdot 10^{-6}$ M, $k_n = 2 \cdot 10^{-5}\ \mathrm{M}^{-1}\ \mathrm{s}^{-1}$, $n_c = 2$, $M(0) = P(0) = 0$. Panel (B) shows the maximal growth rate r_{max}, polymer concentration corresponding to the maximal growth rate M_{max}, time of maximal growth rate t_{max} and lag time τ_{lag}.

Europe PMC Funders Author Manuscripts

Europe PMC Funders Author Manuscripts

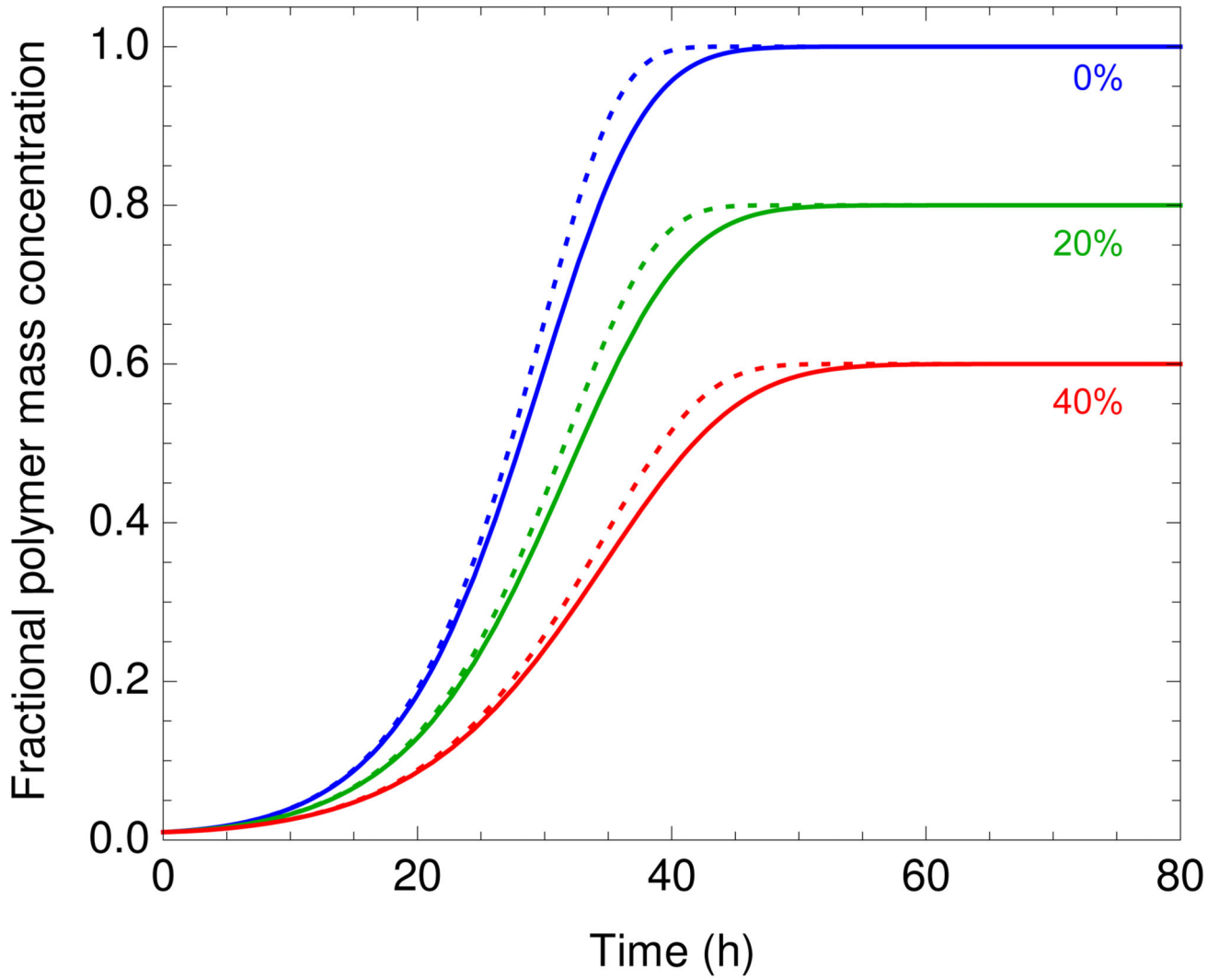

Fig. 5.

Effect of the depolymerisation rate. Sigmoids for increasing depolymerisation rates are shown. Depolymerisation rates are given as a percentage of $k_+ m_{tot}$. In most cases of practical interest [36, 58], $k_{off} \ll k_+ m_{tot}$. Solid lines: first moment $M(t)$ computed from the numerical solution of the master equation Eq. (2). Dashed lines: analytical solution given in Eq. (39). The parameters are: $k_+ = 5 \cdot 10^4\ M^{-1}\ s^{-1}$, $k_- = 2 \cdot 10^{-8}\ s^{-1}$, $m_{tot} = 1 \cdot 10^{-6}$ M, $k_n = 5 \cdot 10^{-5}\ M^{-1}\ s^{-1}$, $n_c = 2$, $M(0) = 1 \cdot 10^{-8}$ M, $P(0) = M(0)/5000$.

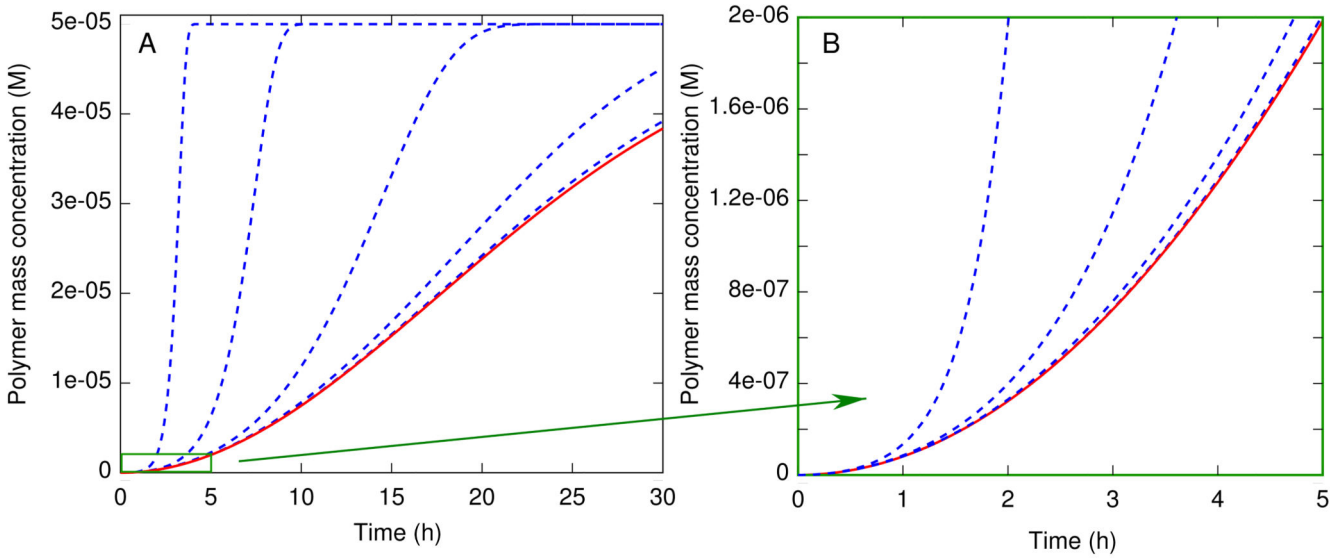

Fig. 6.

Low breakage rate limit, $k_- \rightarrow 0$. Panel A shows Eq. (39) evaluated for successively smaller breakage rates $k_- = 10^{-7}\ s^{-1}$ $k_- = 10^{-8}\ s^{-1}$ $k_- = 10^{-9}\ s^{-1}$ $k_- = 10^{-10}\ s^{-1}$. The other parameters are $k_+ = 5 \cdot 10^4\ M^{-1}\ s^{-1}$, $k_{off} = 0$, $m_{tot} = 50 \cdot 10^{-6}$ M, $k_n = 10^{-6}\ M^{-1}\ s^{-1}$, $M(0) = P(0) = 0$. Panel (B) shows an expanded portion of the $t \rightarrow 0$ limit showing the progressive transition from exponential to polynomial growth (red line, shows Eq. (52)) as a function of time when nucleation takes over from breakage as the most important source of new fibril ends.

Europe PMC Funders Author Manuscripts

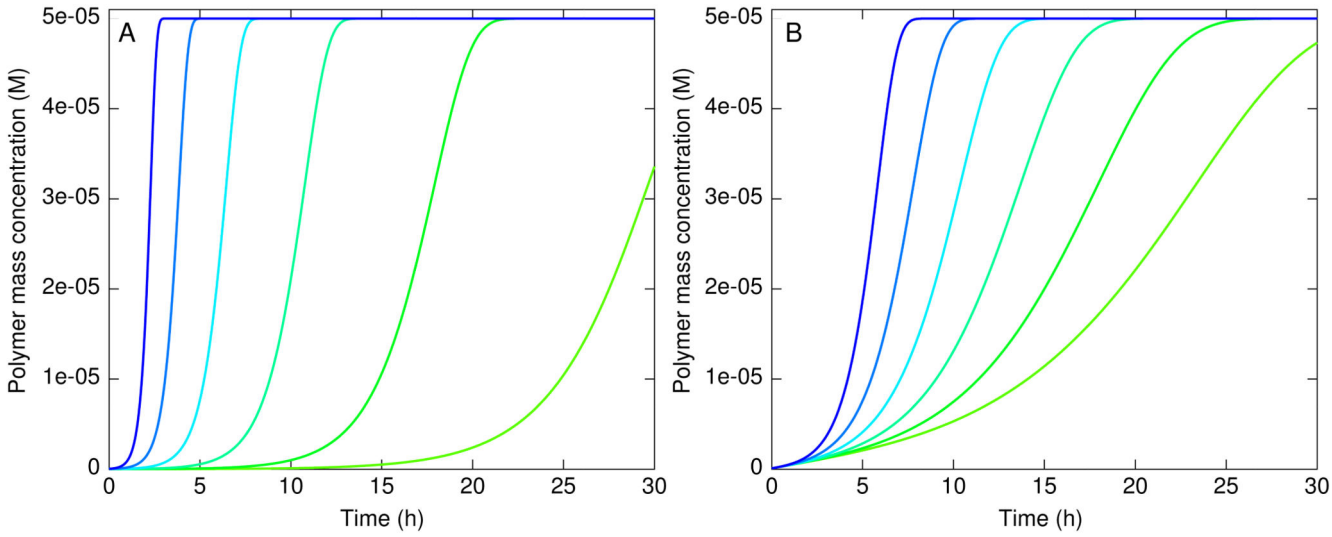

Fig. 7.

Effect of elongation rate and breakage rate on the growth kinetics in the absence of nucleation. In A the elongation rate k_+ is varied, from left to right: $k_+ = 7.3 \cdot 10^5\ M^{-1}\ s^{-1}$, $k_+ = 2.9 \cdot 10^5\ M^{-1}\ s^{-1}$, $k_+ = 1.2 \cdot 10^5\ M^{-1}\ s^{-1}$, $k_+ = 4.7 \cdot 10^4\ M^{-1}\ s^{-1}$, $k_+ = 1.9 \cdot 10^4\ M^{-1}\ s^{-1}$ and $k_+ = 7.5 \cdot 10^3\ M^{-1}\ s^{-1}$ and the other parameters are $k_{off} = 0$, $k_n = 0$, $k_- = 10^{-9}\ s^{-1}$, $m_{tot} = 50\ \mu M$ $M(0) = 1$ nM and $P(0) = M(0)/1000$. In B the breakage rate is varied from left to right: $k_- = 6.4 \cdot 10^{-8}\ s^{-1}$, $k_- = 3.2 \cdot 10^{-8}\ s^{-1}$, $k_- = 1.6 \cdot 10^{-8}\ s^{-1}$, $k_- = 8.0 \cdot 10^{-9}\ s^{-1}$, $k_- = 4.0 \cdot 10^{-9}\ s^{-1}$ and $k_- = 2.0 \cdot 10^{-9}\ s^{-1}$ and the other parameters are: $k_{off} = 0$, $k_n = 0$, $k_+ = 1 \cdot 10^{-4}\ M^{-1}\ s^{-1}$, $m_{tot} = 50\ \mu M$ $M(0) = 1$ nM and $P(0) = M(0)/1000$.

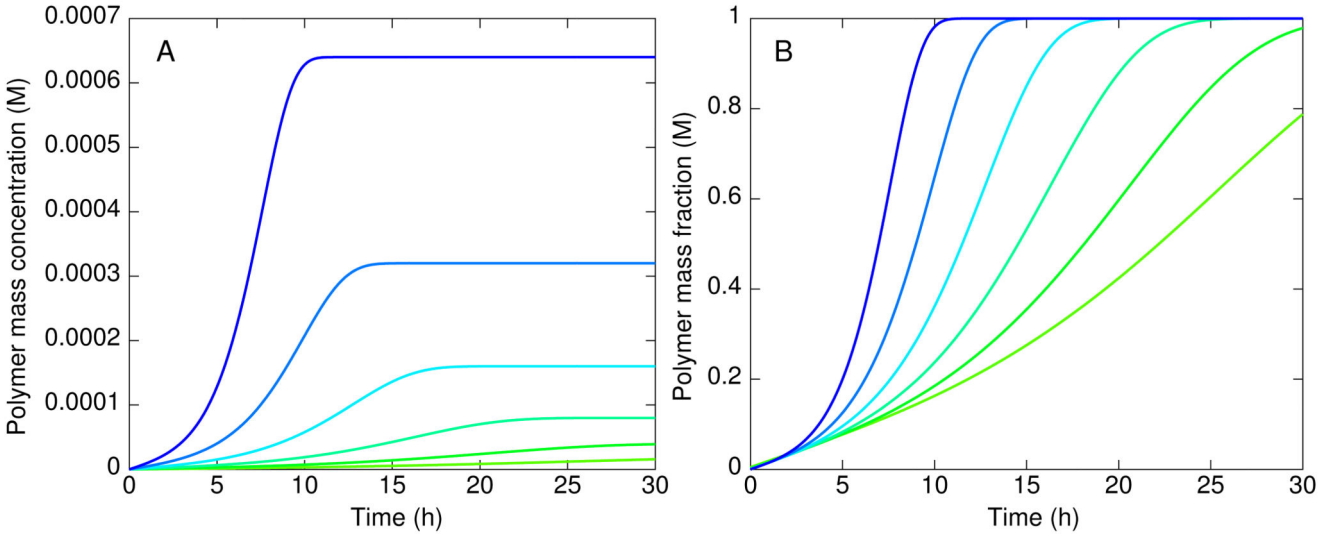

Fig. 8.

Effect of monomer concentration on the growth kinetics in the absence of nucleation. A: Polymer mass concentration $M(t)$ Eq. (39) as a function of time for different total monomer concentrations, from left to right: m_{tot} = 20 μM, m_{tot} = 40 μM, m_{tot} = 80 μM, m_{tot} = 160 μM, m_{tot} = 320 μM and m_{tot} = 640 μM. The values used for the other parameters are: $k_{off} = 0$, $k_n = 0$, $k_+ = 2 \cdot 10^4\ s^{-1}\ M^{-1}$, $k_- = 10^{-9}\ s^{-1}$, $M(0)$ = 100 nM, $P(0) = M(0)/1000$. In B are shown the normalised polymer mass fractions $M(t)/m_{tot}$ as a function of time, for the same monomer concentrations as in A.

Europe PMC Funders Author Manuscripts

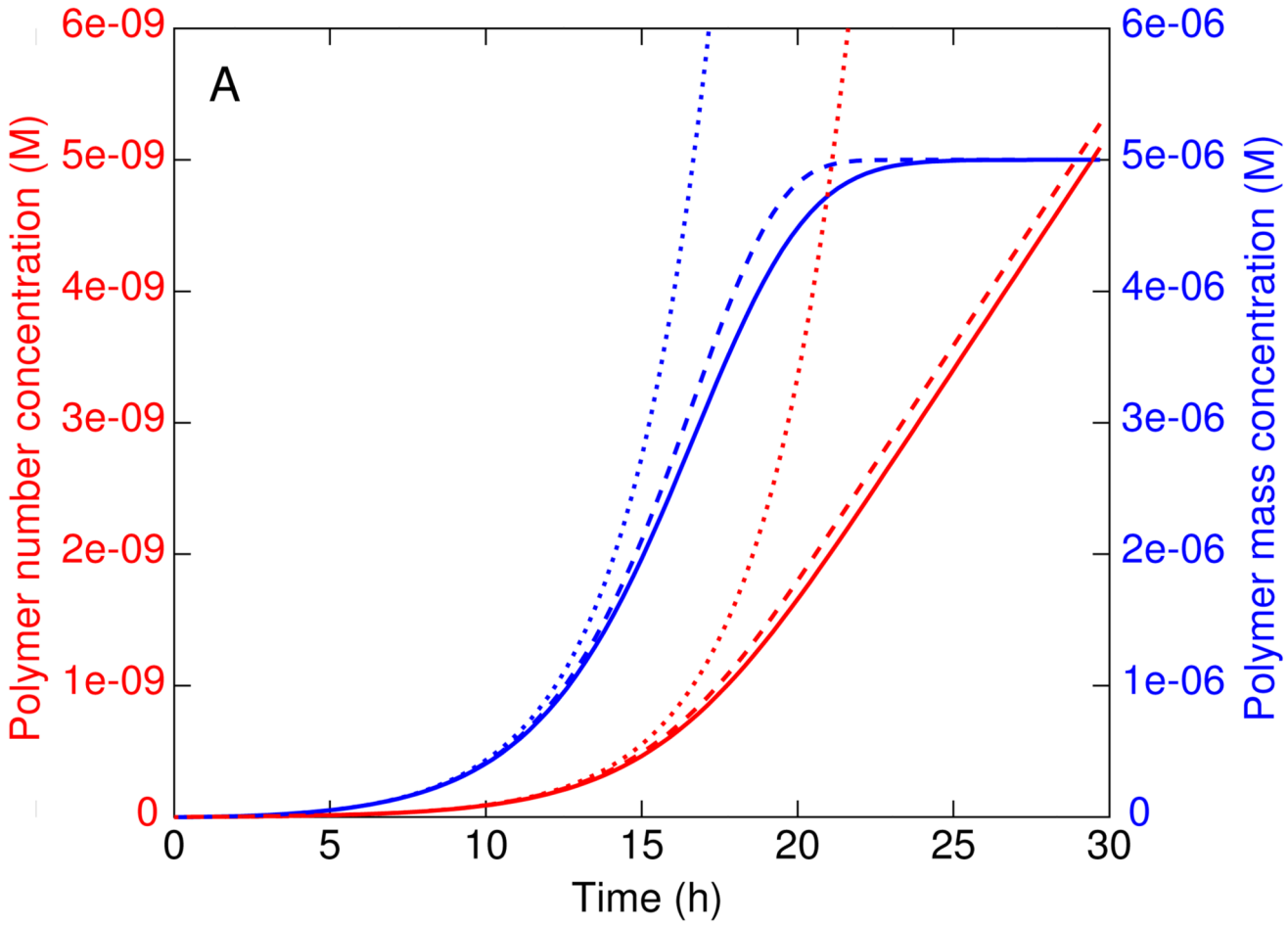

Fig. 9.

Polymer number concentration. The time evolution of the polymer number concentration P (red) from Eq. (56) and mass concentration M (blue) from Fig. 4 are shown for the same parameter values as in Fig. 4. The solid lines show the numerical results, the dashed lines are the analytical solutions and the dotted lines are early time limits from Eqs. (27) and (28).

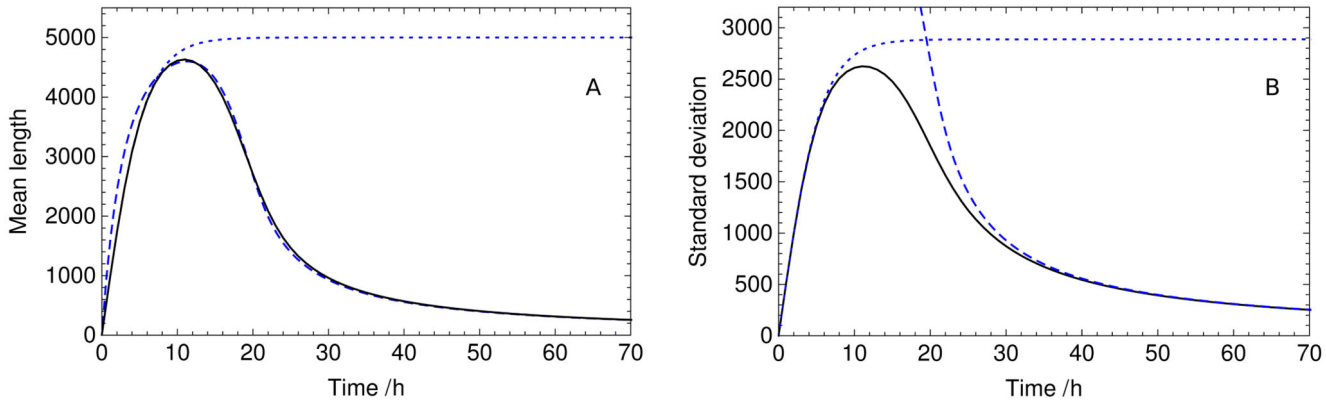

Fig. 10.

Time evolution of the central moments of the filament length distribution. Panel A shows the mean filament length computed numerically (solid black line) and a comparison to the early time linear solution Eq. (58) (dotted blue line) and the full closed-form solution Eq. (61) (dashed blue line). The standard deviation of the length distribution is shown in B. The black line is the result from evaluating the standard deviation from a numerical solution to the master equation Eq. (2), the blue dotted line shows the linear solution valid for early times Eq. (63) and the dashed line shows the approximation $V(t) \sim L(t)$ valid for late times Eq. (64).

Europe PMC Funders Author Manuscripts

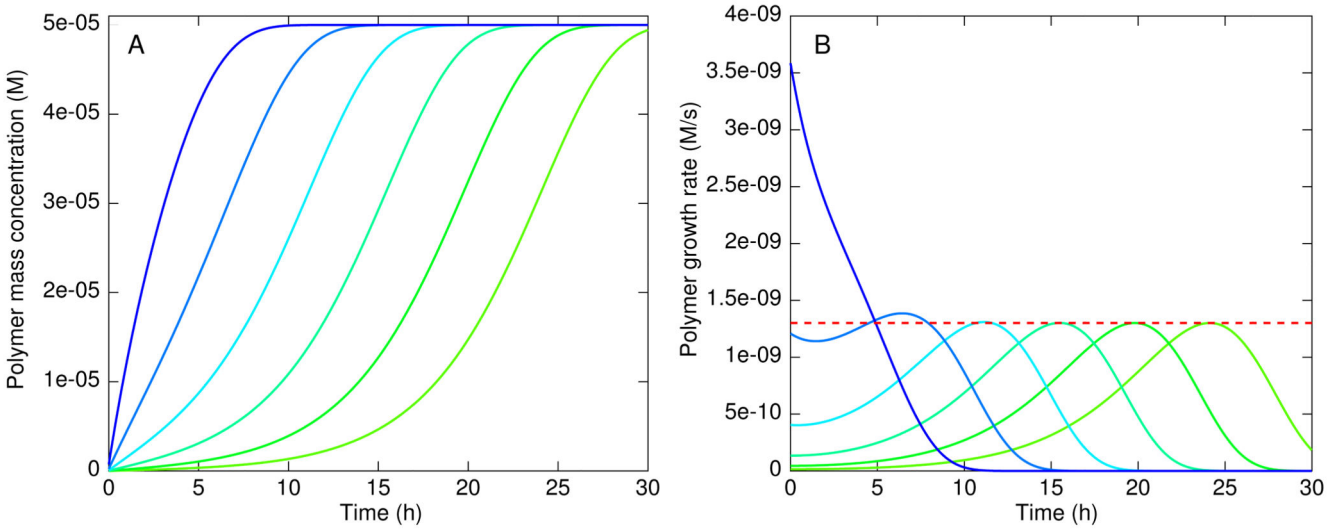

Fig. 11.

Effect of initial seed concentration. A: Polymer mass concentration $M(t)$ Eq. (39) as a function of time for different initial seed concentrations, from left to right: $M(0)$ = 729 nM. $M(0)$ = 243 nM, $M(0)$ = 81 nM, $M(0)$ = 27 nM, $M(0)$ = 9 nM and $M(0)$ = 3 nM, The values used for the other parameters are: $k_{off} = 0$, $k_n = 0$, $k_+ = 5 \cdot 10^4$ s^{-1} M^{-1}, $k_- = 10^{-9}$ s^{-1}, m_{tot} = 50 μM and $P(0) = M(0)/1000$. Panel B shows the growth rate $dM(t)/dt$. Interestingly the maximal growth rate is independent of the seed concentration, except for seed concentrations that are higher than the critical concentration (M_c = 260 nM for the parameters used) as described in the text. The maximal growth rate Eq. (78) ($1.3 \cdot 10^{-9}$ for the parameters used) is shown as a dashed red line.

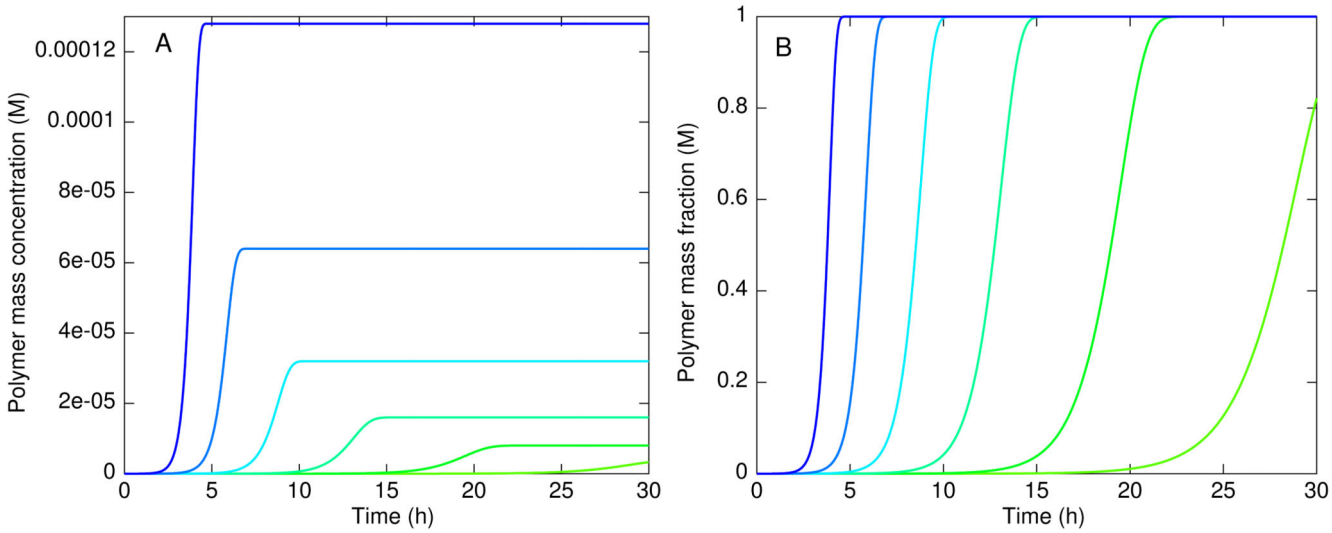

Fig. 12.

Nucleated growth with varying monomer concentrations. A: Polymer mass concentration $M(t)$ Eq. (39) as a function of time for different total monomer concentrations, from left to right: $m_{tot} = 1.3 \cdot 10^{-4}$ M, $m_{tot} = 6.4 \cdot 10^{-5}$ M, $m_{tot} = 3.2 \cdot 10^{-5}$ M, $m_{tot} = 1.6 \cdot 10^{-5}$ M, $m_{tot} = 8.0 \cdot 10^{-6}$ M, $m_{tot} = 4.0 \cdot 10^{-6}$ M. The values used for the other parameters are: $k_{off} = 0$, $n_c = 2$, $k_n = 10^{-8}$ M^{-1} s^{-1}, $k_+ = 5 \cdot 10^4$ s^{-1} M^{-1}, $k_- = 5 \cdot 10^{-8}$ s^{-1}, $M(0) = P(0) = 0$. In B are shown the normalised polymer mass fractions $M(t)/m_{tot}$ as a function of time, for the same monomer concentrations as in A.

Europe PMC Funders Author Manuscripts

Europe PMC Funders Author Manuscripts

Table I

Comparison of the first order self-consistent solutions for irreversible filament growth with secondary nucleation or fragmentation with the analogous results from the theory of nucleated polymerisation

	Nucleated polymerisation (see Appendix)	Breakable filaments	Secondary nucleation
Parameters	k_n, n_c, k_+, m_{tot}	k_n, n_c, k_+, k_-, m_{tot}	k_n, n_c, k_2, n_2, k_+, m_{tot}
Polymer mass $\frac{M(t)}{m_{tot}} =$	$1-\frac{m(0)}{m_{tot}}\left[\mu\,\mathrm{sech}\left(\nu+\lambda_0\,\beta^{-\frac{1}{2}}\mu t\right)\right]^{\beta}$	$1-\exp\left(-C_+e^{-\kappa t}+C_-e^{-\kappa t}+\frac{\lambda_0^2}{\kappa^2}\right)$	$1-\exp\left(-C_+e^{\kappa t}+C_-e^{-\kappa t}+\frac{\lambda_0^2}{\kappa^2}\right)$
	$\lambda_0=\sqrt{2k_+k_n m(0)^{n_c}}\quad \beta=2/n_c$	$\kappa=\sqrt{2k_+k_-m(0)}$	$\kappa=\sqrt{2k_+k_2 m(0)^{n_2+1}}$
	$\gamma=\frac{\beta^{1/2}k_+n_c}{\lambda_0}P(0)\quad \mu=\sqrt{1+\gamma^2}\quad \nu=\mathrm{arsinh}\,(\gamma)$	$C_\pm=\frac{k_+P(0)}{\kappa}\pm\frac{M(0)}{2m(0)}\pm\frac{\lambda_0^2}{2\kappa^2}$	$C_\pm=\frac{k_+P(0)}{\kappa}\pm\frac{M(0)}{2m(0)}\pm\frac{\lambda_0^2}{2\kappa^2}$
Early time behaviour $M(t) \approx$	$\frac{1}{2}m_{tot}\lambda_0^2 t^2$	$m_{tot}(C_+e^{\kappa t}-C_-e^{-\kappa t})$	$m_{tot}(C_+e^{\kappa t}-C_-e^{-\kappa t})$
Lag time $\tau_{lag} =$	$\left[\mathrm{artanh}\left(\sqrt{\frac{n_c}{2+n_c}}\right)-\nu-\frac{m_{tot}-m(0)\mu^{\frac{2}{n_c}}\left(\frac{4+4n_c}{(2+n_c)^2}\right)^{\frac{1}{n_c}}}{\frac{2m(0)}{\sqrt{n_c(2+n_c)}}\left(\frac{2\mu^2}{2+n_c}\right)^{\frac{1}{n_c}}}\right]\beta^{\frac{1}{2}}(\mu\lambda_0)^{-1}$	$[\log(C_+)-e+1]\kappa^{-1}$	$[\log(C_+)-e+1]\kappa^{-1}$
Approximate lag time exponent $\gamma =$	$-n_c/2$	$-1/2$	$-(n_2+1)/2$
Maximal growth rate $r_{max} =$	$\frac{2m(0)}{\sqrt{n_c(2+n_c)}}\left(\frac{2\mu^2}{2+n_c}\right)^{\frac{1}{n_c}}\beta^{-\frac{1}{2}}\mu\,\lambda_0$	$m_{tot}\frac{\kappa}{e}$	$m_{tot}\frac{\kappa}{e}$